Semi-annual Progress Report
SURI No. 1188-33
(SUSASL No. 33)

STABILITY OF CYLINDRICAL SHELLS

AN ANALYTICAL AND EXPERIMENTAL INVESTIGATION OF THE EFFECTS OF LARGE PREBUCKLING DEFORMATIONS ON THE BUCKLING OF CLAMPED THIN-WALLED CYLINDRICAL SHELLS SUBJECTED TO AXIAL LOADING AND INTERNAL PRESSURE

by

Dannie Gorman

Sponsor: National Aeronautics and Space Administration (NASA)

NASA Grant No. NsG-627/33-22-010

For Period: October 1, 1964 - March 31, 1965

Project Director: R. M. Evan-Iwanowski

SYRACUSE UNIVERSITY RESEARCH INSTITUTE
Department of Mechanical & Aerospace Engineering
APPLIED MECHANICS LABORATORY

N 23649

Abstract

An analytical and experimental investigation of the effects of large prebuckling deformation on the buckling of thin-walled, clamped, cylindrical shells subjected to combinations of axial loading and internal pressure, has been carried out. These large deformations are caused by edge conditions at the ends of the shells.

Imperfection free test specimens have been provided by the centrifugal casting of a birefringent eppoxy resin compound. A carefully executed test program permitted achievement of a one-to-one correspondence between the theoretical and experimental models. The existence of the prebuckling deformations has been demonstrated by means of the photoelastic (photostress) technique. A "two-step" perturbation technique has been used to arrive at the differential equations governing the shell buckling and a solution has been achieved by means of the Galerkin method and application of the IBM 7074 computer.

The role of the nonuniform deformation, in reducing the buckling loads from that predicted by classical linear theory, has been demonstrated by experiment. Good agreement between analysis and experiment has been encountered for shells of limited range of shell lengths.

The inadequacy of the classical membrane model to describe such shells at the incipience of buckling is verified.

Author

Preface

The objective of this work has been to demonstrate both analytically and experimentally the effect of large nonuniform prebuckling deformations on the buckling of clamped thin-walled, cylindrical shells subjected to combinations of axial compressive loading and internal pressure. These prebuckling deformations arise due to the clamped conditions imposed at the edges of the shells.

The urgent need for such an investigation resulted from recent analytical research work carried out in this field by Stein[15] and Fischer.[16] They investigated the effects of large prebuckling deformations on the buckling loads of simply supported cylindrical shells. Stein reported reductions of up to 55% from the buckling loads predicted by classical linear theory. Fischer reported reductions of not more than 15%. Koiter[17] pointed out that the difference in their findings was probably due in part to the fact that Stein studied the case of vanishing tangential shear at the edges, while Fischer studied the case of vanishing tangential displacement. He also pointed out that Stein's edge conditions did not correspond to those used in the classical linear theory.

It thereby became apparent, that the ultimate answer to the question regarding the role of prebuckling deformations in reducing the buckling loads of thin cylinders would have to be sought in careful experiment. Coupled with this experimental work, an analysis would have to be carried out which provided a one-to-one correspondence with the experiment.

The test specimens have been prepared from a birefringent eppoxy resin compound by means of the centrifugal casting technique. Shells have been found to be virtually free of initial geometrical imperfections and the isolation of the effects of the prebuckling deformations in reducing buckling loads from that predicted by classical linear theory has therefore been made possible. Shells have been tested with ratios of radius to thickness varying from 133 to 200, and ratios of length to radius from 0.75 to 4.3. The existence of the prebuckling deformations has been demonstrated by means of the photoelastic (photostress) technique.

The nonlinear Donnell equilibrium equations have been used in the analysis. A solution for the prebuckling problem has been achieved and a "two-step" perturbation technique has been used to arrive at the differential equations governing the shell buckling.

The buckling equations have been solved by means of the Galerkin method and with the aid of an IBM 7074 digital computer.

Results of both the experimental and analytical work have been presented in graphical form and these findings have been discussed at some length.

This work has been sponsored by the National Aeronautics and Space Administration, Grant NsG-627.

It has also been supported in part by the National Science Foundation Grant GP-137.

TABLE OF CONTENTS

LIST OF FIGURES

LIST OF SYMBOLS

D	Flexural rigidity of shell wall = $\dfrac{Et^3}{12(1-\nu^2)}$
E	Young's modulus
J	Number of peripheral waves around the buckled shell
K	Number of terms employed in trigonometric expansions
L	Shell length
ℓ	Shell half-length
M_x, M_y, M_{xy}	Resultant bending and twisting moments in shell wall
$N_x, N_y, N_{xy}, Q_x, Q_y$	Shell wall longitudinal and shear stress resultants
p	Internal pressure
P	Axial loading per unit circumference along shell edge
P_E	Axial loading per unit circumference along shell edge at classical (Euler) buckling load
P^*	P/P_E
p^*	Ratio of hoop stress due to internal pressure, to axial buckling stress based on classical theory
R	Mean radius of shell
t	Thickness of shell wall
u^*, v^*, w^*	Displacements in the x,y, and radial outward directions respectively
$\bar{u}$, $\bar{w}$	Prebuckling displacements
u, v, w	Displacements associated with buckling
U, V, W	Functions of "x" used to express the buckling displacements
x,y	Axial and circumferential directions
Z	Shell parameter $\frac{L^2}{Rt}\sqrt{(1-\nu^2)}$

∇^4	$\frac{\partial^4}{\partial x^4} + 2\frac{\partial^4}{\partial x^2 \partial y^2} + \frac{\partial^4}{\partial y^4}$
ϵ_x, ϵ_y, γ_{xy}	Longitudinal strains in x and y directions, and shear strain
ν	Poisson's ratio
ξ	Distance from edge of shell
τ_{max}	Maximum shear stress in prebuckled shell wall = $(N_x - N_y)/2t$
τ_F	Maximum shear stress in prebuckled shell neglecting edge effects

INTRODUCTION

The mathematical foundations of the theory of elastic stability were first laid down by Euler. On the basis of this theory Timoshenko[1] computed the buckling loads for thin cylindrical shells subjected to axial loading.

Choosing a suitable coordinate system to specify the shell initial configuration, he equated to zero the resultants of the longitudinal, tangential, and radial forces acting on a differential element of the shell. Using Hook's law to relate stresses with strains, and the linearized strain displacement relationships, he arrived at three simultaneous linear homogeneous differential equations of equilibrium relating the shell displacements, end loading, shell structural properties and geometry.

It was assumed that on buckling the shell generators and circumference take on a sinusoidal configuration. The small longitudinal, tangential, and radial displacements were assumed to be of the form (Fig. 3)

$$u^* = A \sin \frac{ny}{R} \cos \frac{m\pi x}{L}$$

$$v^* = B \cos \frac{ny}{R} \sin \frac{m\pi x}{L}$$

$$w^* = C \sin \frac{ny}{R} \sin \frac{m\pi x}{L}$$

with the origin of coordinates taken at one end of the shell. These displacements required that the shell generators divide into m half waves, and the circumference into n full waves. Substituting these expressions for the displacements into the differential equations of equilibrium he arrived at a set of three simultaneous algebraic linear homogeneous equations for the quantities A, B, and C. To compute the buckling load it was required that a non-trivial solution exist for these quantities, i.e., that the determinant of their coefficient matrix be equal to zero. This put a relationship between the shell loading and the integers n, and m. It was then shown that the lowest value of the loading which could satisfy the constraining relationship, with permissible values of m and n was as follows:

$$P_E = \frac{Et^2}{R\sqrt{3(1-\nu^2)}}$$

where P_E is known as the Euler buckling load per unit circumference along the edge of the shell.

In the case of columns and plates, very good agreement has been found between predictions based on theory and experimental results, however, in the case of thin walled cylindrical shells subjected to axial compressive loading, large discrepancies have been encountered. In experiments carried out by Donnell[2] and others[3] it was found that these shells buckled under loads of only a fraction of that predicted by theory (Fig. 1).

Donnell[2], and later Donnell and Wan[4], tried to explain this discrepancy on the existence of geometric imperfections as well as residual stresses in the test specimens. Flügge[5] attempted to explain it by attributing it to the restraint to radial movement of the shells which was provided by the testing machine or supporting edge plates. Both were able to explain a certain amount of reduction in the critical buckling load, however, they could not account for the fact that the configuration of the buckled test shell was much different from that predicted by theory.

The reason why thin cylindrical shells do not behave in a manner similar to flat plates when they buckle was investigated by von Kármán and Tsien[6]. They showed that on buckling, thin shells can undergo lateral deformations of the order of several wall thicknesses. The relationships which then connect the displacements with the stresses are highly nonlinear. A nonlinear large deflection theory must therefore be used instead of the linear one. The nonlinear theory was laid down by Donnell[2], and von Kármán and Tsien employed it to determine the possible equilibrium configurations of a thin cylindrical shell under axial loading. A deformation form of the type observed in buckled shells was assumed and the Rayleigh-Ritz method was used to obtain a solution.

Von Kármán and Tsien found that there existed other equilibrium configurations in addition to the unbuckled configuration, for loads lower than the Euler critical load (Fig. 2). These other configurations were associated with large deflections in the cylinder walls. While this approach did not indicate that shells must buckle at loads lower than the Euler load it did show that small external disturbances could readily cause shells to "jump" from an unbuckled to a nearby buckled configuration before the Euler load had been reached.

A valuable contribution to the understanding of why experimentally observed large displacement buckling is possible with thin cylindrical shells was made by Yoshimura[7]. He used differential geometry to show that a circular cylindrical shell could be transformed into a set of plane triangles. This transformation required bending of the shell wall. The work of bending of a thin shell wall is relatively small compared to that of membrane compression or extension. This explained the ability of the walls to undergo large displacements due to bending. In contrast, flat plates with edges supported against lateral displacements cannot be deformed to a large deflection buckled configuration without large membrane strains occurring and hence much additional work being supplied by the applied load. The ability of plates to carry increased loads after buckling without undergoing large deformation is thus explained.

In reviewing the extensive literature available on the subject of buckling of thin cylindrical shells it is surprising to find that so little attention has been devoted to investigating the effects of edge conditions on the buckling loads. An explanation, perhaps, may be found in the experimental results obtained by earlier writers.[2] In many cases it has been assumed that a shell whose length is greater than three quarters of its diameter may be considered as a shell of infinite length in so far as edge effects are concerned. In other cases the edges are considered to be supported in some way during buckling but prebuckling deformation is either neglected or considered to be uniform throughout and prebuckling bending stresses are assumed to have no effect on the buckling load. These assumptions, convenient though they may be from the viewpoint of the analysis, have been seriously challenged by more recent researchers in this field.

Thielmann[8] has criticized the assumption of von Kármán and Tsien, and of later researchers, that buckles are distributed periodically over the entire length of the buckled shell and that shell length has no influence on buckling loads. This assumption has been made in spite of the fact that in experimental tests local buckles are observed. In more recent works by Uemura[9], and Evan-Iwanowski[10] the phenomena of localized buckling has been introduced.

In reviewing papers in connection with experimental work carried out by Donnell[2] one finds the following statement with regard to edge conditions, "In all the experiments cited in this paper the ends of the cylinders were clamped or fixed in some way. This stabilized the wall of the cylinder near the ends to such an extent that buckling always started at some distance from the ends. When cylinders are tested free ended, eccentricity of loading and other local conditions at the ends are likely to obtain." In a recent report by Tennyson[11] it has been claimed that imperfection free cylindrical shells can be made to buckle arbitrarily close to the classical buckling load, with limiting factors being the degree of precision and care used in testing. Leonard[12] has completely disagreed with this claim. The following is a quotation from his remarks on the matter, "The author is completely disregarding an important source of error in the classical theory which is entirely unrelated to initial shape imperfections: the inconsistent assumption made in classical theory regarding edge conditions."

A solution to the linearized axisymmetric prebuckling deformation problem for a shell with simply supported edges has been provided by Föppl[13] and is presented by Flügge[4]. Stein[15] computed the solution for the nonlinear problem of prebuckling deformations of simply supported cylindrical shells and he computed buckling loads by considering the shell to buckle from this initial nonuniform deformation configuration. He found that the buckling loads were now as little as 45% of those predicted by classical theory.

Fischer[16] has investigated a similar problem and has found reduction from the Euler buckling loads, due to prebuckling deformations of about 15%. Koiter[17] has pointed out that the differences in Stein's and Fischer's work may be explained in part by the fact that Fischer used the condition of vanishing tangential displacement at the edges while Stein used the condition of vanishing tangential shear. He also stated that since the conditions of Fischer represent those used in the classical membrane problem, a reduction in critical load for Stein's condition of zero tangential shear would likely be obtained even in the case of the membrane solution if Stein's boundary conditions were used. This was shown to be the case by Ohira[21] and by Hoff and Rehfield,[22].

Recently, Hoff[18] has presented a solution for the axisymmetric buckling of the free end of a thin cylindrical shell. Subsequently Nachbar and Hoff[19] have presented a solution to the same type of problem where buckling deformations have not been restricted to the axisymmetric case. In both instances buckling loads well below the Euler loads have been computed.

The objective set forth in this thesis has been to resolve both experimentally and analytically the effects of prebuckling stresses and deformations on the buckling of thin cylindrical shells with clamped edges. It became evident in the early stages of the work that in order to isolate the edge effects experimentally it would be necessary to fabricate test specimens which were virtually free of initial geometric imperfections as well as residual stresses. It furthermore became evident that extreme caution would have to be exercised in fabricating and fitting edge clamping plates, as well as in applying loading to the shells, so that all other possible sources of reduction in buckling loads from the Euler loads would be minimized. In this manner only, could the reduction in buckling loads due to edge effects be determined.

In seeking an analytical solution to this buckling problem it became apparent that the solution must be one which satisfied completely the prescribed experimental boundary conditions. A one-to-one correspondence, thus, between experimental boundary conditions and those formulated mathematically would have to be satisfied. In this manner the reduction in buckling load from the Euler load, due to the effects of clamped edges, would be properly evaluated.

Analytical Procedure

The Equilibrium Equations

In order to take into consideration the effects of prebuckling deformations on the buckling of shells, the "two-step" perturbation technique used by Stein[15] to arrive at the differential equations governing the buckling is employed here. The large deflection solution for the case of a thin simply supported cylindrical shell subjected to axial and uniform lateral loading, has been provided by Stein[15]. The solution for the case of a shell with clamped edge conditions has been computed and is presented here. In both cases the Donnell large deflection equations[20] have been used. For completeness a brief review of the development of these equations is presented below.

Referring to Fig. 3 and writing the equations of equilibrium for the forces acting in the x, y, and radial directions respectively we have:

$$\frac{\partial N_x}{\partial x} + \frac{\partial N_{xy}}{\partial y} = 0 \qquad \text{(a)}$$

$$\frac{\partial N_{xy}}{\partial x} + \frac{\partial N_y}{\partial y} = 0 \qquad \text{(b)}$$

$$\frac{\partial Q_x}{\partial x} + \frac{\partial Q_y}{\partial y} + \frac{N_y}{R} - \left(N_x \frac{\partial^2 w}{\partial x^2} + N_y \frac{\partial^2 w}{\partial y^2} + 2N_{xy} \frac{\partial^2 w}{\partial x \partial y}\right) = p \qquad \text{(c)} \qquad (1)$$

The equilibrium equations for the moments about the x, and y axis respectively are

$$\frac{\partial M_y}{\partial y} + \frac{\partial M_{xy}}{\partial x} - Q_y = 0 \qquad \text{(d)}$$

$$\frac{\partial M_x}{\partial x} + \frac{\partial M_{xy}}{\partial y} - Q_x = 0 \qquad \text{(e)}$$

Using the relations

$$M_x = \frac{Et^3}{12(1-\nu^2)} \left(\frac{\partial^2 w^*}{\partial x^2} + \nu \frac{\partial^2 w^*}{\partial y^2}\right) \quad , \quad M_y = \frac{Et^3}{12(1-\nu^2)} \left(\frac{\partial^2 w^*}{\partial y^2} + \nu \frac{\partial^2 w^*}{\partial x^2}\right)$$

and

$$M_{xy} = \frac{Et^3}{12(1+\nu)} \frac{\partial^2 w^*}{\partial x \partial y}$$

We may write from Eqs. (1)d, (1)e

$$\frac{\partial Q_y}{\partial y} + \frac{\partial Q_x}{\partial x} = \frac{\partial^2 M_y}{\partial y^2} + \frac{\partial^2 M_{xy}}{\partial y \partial x} + \frac{\partial^2 M_x}{\partial x^2} + \frac{\partial^2 M_{xy}}{\partial y \partial x}$$

$$= \frac{Et^3}{12(1-\nu^2)} \left[\left(\frac{\partial^4 w^*}{\partial y^4} + \nu \frac{\partial^4 w^*}{\partial y^2 \partial x^2}\right) + \left(\frac{\partial^4 w^*}{\partial x^4} + \nu \frac{\partial^4 w^*}{\partial x^2 \partial y^2}\right) + 2 \left(\frac{\partial^4 w^*}{\partial x^2 \partial y^2} - \nu \frac{\partial^4 w^*}{\partial x^2 \partial y^2}\right)\right]$$

$$= D \nabla^4 w^*$$

Substituting in Eq. (1)c, we now have for the set of Donnell equilibrium equations

$$\frac{\partial N_x}{\partial x} + \frac{\partial N_{xy}}{\partial y} = 0 \qquad \text{(a)}$$

$$\frac{\partial N_y}{\partial y} + \frac{\partial N_{xy}}{\partial x} = 0 \qquad \text{(b)} \quad (2)$$

$$D\nabla^4 w^* + \frac{N_y}{R} - \left(N_x \frac{\partial^2 w}{\partial x^2} + 2N_{xy} \frac{\partial^2 w}{\partial x \partial y} + N_y \frac{\partial^2 w}{\partial y^2}\right) = p \qquad \text{(c)}$$

From Hook's law we have

$$N_x = \frac{Et}{(1-\nu^2)} (\varepsilon_x + \nu\varepsilon_y) \qquad \text{(a)}$$

$$N_y = \frac{Et}{(1-\nu^2)} (\varepsilon_y + \nu\varepsilon_x) \qquad \text{(b)} \quad (3)$$

$$N_{xy} = \frac{Et}{2(1+\nu)} \gamma_{xy} \qquad \text{(c)}$$

The nonlinear relationships connecting strains and displacements are,

$$\varepsilon_x = \frac{\partial u^*}{\partial x} + \frac{1}{2} \left(\frac{\partial w^*}{\partial x}\right)^2 \qquad \text{(a)}$$

$$\varepsilon_y = \frac{\partial v^*}{\partial y} + \frac{w^*}{R} + \frac{1}{2} \left(\frac{\partial w^*}{\partial y}\right)^2 \qquad \text{(b)} \quad (4)$$

$$\gamma_{xy} = \frac{\partial u^*}{\partial y} + \frac{\partial v^*}{\partial x} + \frac{\partial w^*}{\partial x} \frac{\partial w^*}{\partial y} \qquad \text{(c)}$$

The Prebuckling Deformation

In view of the axial symmetry of the prebuckling problem, it is obvious that both terms on the left hand side of (2)b, are identically zero. Also u and v are functions of x only.

Substituting expressions for stresses in terms of displacements we have from (3)a,

$$N_x = -P = \frac{Et}{(1-\nu^2)}\left[\frac{du^*}{dx} + \frac{\nu w^*}{R} + \frac{1}{2}\left(\frac{dw^*}{dx}\right)^2\right] \tag{5}$$

and from (2)c,

$$\frac{d^4w^*}{dx^4} + \frac{12P}{Et^3}(1-\nu^2)\frac{d^2w^*}{dx^2} + \frac{12}{R^2t^2}w^* + \frac{12\nu}{Rt^2}\frac{du^*}{dx} + \frac{6\nu}{Rt^2}\left(\frac{dw^*}{dx}\right)^2 = \frac{12p(1-\nu^2)}{Et^3} \tag{6}$$

Substituting (5) in (6) we obtain

$$\frac{d^4w^*}{dx^4} + \frac{P^2}{D}\frac{d^2w^*}{dx^2} + \frac{Et}{R^2D}w^* = \frac{p}{D} + \frac{P}{DR} \tag{7}$$

The solution to (7) for the case of clamped edges, i.e., $w^* = dw^*/dx = 0$ at $x = \pm L/2$, has been computed and is as follows:

$$w^* = C_1 \sin\theta x \sinh\phi x + C_2 \cos\theta x \cosh\phi x + q \tag{8}$$

where,

$$q = \frac{R}{Et}\left(p + \frac{\nu P}{R}\right) \quad ; \quad \theta = \frac{1}{2L}\sqrt{4\sqrt{3}z + \frac{PL^2}{D}}$$

$$\phi = \frac{1}{2L}\sqrt{4\sqrt{3}z - \frac{PL^2}{D}}$$

$$C_1 = -2q \frac{\theta \sin \frac{\theta L}{2} \cosh \frac{\phi L}{2} - \phi \cos \frac{\theta L}{2} \sinh \frac{\phi L}{2}}{\theta \sinh \phi L + 2\phi \sin \frac{\theta L}{2} \cos \frac{\theta L}{2}}$$

$$C_2 = -2q \frac{\phi \sin \frac{\theta L}{2} \cosh \frac{\phi L}{2} + \theta \cos \frac{\theta L}{2} \sinh \frac{\theta L}{2}}{\theta \sinh \phi L + 2\phi \sin \frac{\theta L}{2} \cos \frac{\theta L}{2}}$$

differentiating with respect to x, we obtain

$$\frac{dw^*}{dx} = \gamma_1 \sin \theta x \cosh \phi x + \gamma_2 \cos \theta x \sinh \phi x$$

and

$$\frac{d^2w^*}{dx^2} = \gamma_3 \sin \theta x \sinh \phi x + \gamma_4 \cos \theta x \cosh \phi x$$

where

$$\gamma_1 = C_1\phi - C_2\theta \qquad \gamma_2 = C_2\phi + C_1\theta$$

$$\gamma_3 = \gamma_1\phi - \gamma_2\theta \qquad \gamma_4 = \gamma_2\phi + \gamma_1\theta$$

The solution for the axisymmetric prebuckled form when P is greater than P_E (the Euler loading), that is when the quantity $\sqrt{4\sqrt{3}z - \frac{PL^2}{D}}$ becomes imaginary, may be expressed as follows

$$w^* = C_1 \sin \theta x \sin \phi x + C_2 \cos \theta x \cos \phi x + q \tag{9}$$

where q is unchanged but where,

$$C_1 = -q \frac{[\theta \cos \frac{\phi L}{2} \sin \frac{\theta L}{2} + \phi \cos \frac{\theta L}{2} \sin \frac{\phi L}{2}]}{[\theta \sin \frac{\phi L}{2} \cos \frac{\phi L}{2} + \phi \sin \frac{\theta L}{2} \cos \frac{\theta L}{2}]}$$

$$C_2 = -q \frac{[\theta \cos \frac{\theta L}{2} \sin \frac{\phi L}{2} + \phi \sin \frac{\theta L}{2} \cos \frac{\phi L}{2}]}{[\theta \sin \frac{\phi L}{2} \cos \frac{\phi L}{2} + \phi \sin \frac{\theta L}{2} \cos \frac{\theta L}{2}]}$$

and where

$$\theta = \frac{1}{2L} \sqrt{\frac{PL^2}{D} + 4\sqrt{3}z} \qquad \phi = \frac{1}{2L} \sqrt{\frac{PL^2}{D} - 4\sqrt{3}z}$$

The Buckling Problem

Before beginning the calculation of the buckling loads, a consideration of the applicable boundary conditions to be satisfied during buckling is in order. There exist many sets of boundary conditions which are commonly referred to as simply supported or clamped conditions. Four sets of each condition have been discussed in Ref. [24] and are presented here as examples.

Simply support conditions:

(1) $w^* = M_{x1} = N_{x1} = v^* = 0$

(2) $w^* = M_{x1} = N_{x1} = N_{xy1} = 0$

(3) $w^* = M_{x1} = u^* = N_{xy1} = 0$

(4) $w^* = M_{x1} = u^* = v^* = 0$

Clamped boundary conditions:

(1) $$w^* = \frac{\partial w^*}{\partial x} = N_{x1} = v^* = 0$$

(2) $$w^* = \frac{\partial w^*}{\partial x} = N_{x1} = N_{xy1} = 0$$

(3) $$w^* = \frac{\partial w^*}{\partial x} = u^* = N_{y1} = 0$$

(4) $$w^* = \frac{\partial w^*}{\partial x} = u^* = v^* = 0$$

Subscripts 1 indicate incremental stress resultants due to buckling. The edge conditions used in buckling tests referred to in this thesis are described by condition (4) in the "clamped boundary conditions" i.e.

$$w^* = \frac{\partial w^*}{\partial x} = u^* = v^* = 0$$

In order to arrive at the differential equations governing the buckling of the shell we add to the prebuckling displacements the infinitesimal buckling displacements u, v, and w. The total displacements, denoted u*, v* and w* may thus be written as

$$\begin{aligned} u^* &= \bar{u} + u(x,y) \\ v^* &= v(x,y) \\ w^* &= \bar{w} + w(x,y) \end{aligned} \tag{10}$$

Expressing the three equilibrium equations in terms of these displacements and dropping terms which are products of the infinitesimal buckling displacements u, v, and w, and making use of expressions involving prebuckling deformations we arrive at the following equilibrium equations[15]:

$$\frac{\partial^2 u}{\partial x^2} + \frac{1-\nu}{2}\frac{\partial^2 u}{\partial y^2} + \frac{(1+\nu)}{2}\frac{\partial^2 v}{\partial x \partial y} + \frac{\nu}{R}\frac{\partial w}{\partial x} + \frac{\partial}{\partial x}\left(\frac{\partial \bar{w}}{\partial x}\frac{\partial w}{\partial x}\right)$$

$$+ \frac{(1-\nu)}{2}\frac{d\bar{w}}{dx}\frac{\partial^2 w}{\partial y^2} = 0$$

$$\frac{(1+\nu)}{2}\frac{\partial^2 u}{\partial x \partial y} + \frac{\partial^2 v}{\partial y^2} + \frac{(1-\nu)}{2}\frac{\partial^2 v}{\partial x^2} + \frac{1}{R}\frac{\partial w}{\partial y} + \frac{(1-\nu)}{2}\frac{d^2\bar{w}}{dx^2}\frac{\partial w}{\partial y}$$

$$+ \frac{(1+\nu)}{2}\frac{\partial \bar{w}}{\partial x}\frac{\partial^2 w}{\partial x \partial y} = 0 \qquad (11)$$

$$D\nabla^4 w + \frac{1}{R}N_{yB} + P\frac{\partial^2 w}{\partial x^2} + \nu P\frac{\partial^2 w}{\partial y^2} - \frac{Et}{R}\frac{\bar{w}\partial^2 w}{\partial y^2} - \frac{d^2\bar{w}}{dx^2}N_{xB} = 0$$

where

$$N_{xB} = \frac{Et}{1-\nu^2}\left[\frac{\partial u}{\partial x} + \frac{d\bar{w}}{dx}\frac{\partial w}{\partial x} + \nu\left(\frac{\partial v}{\partial y} + \frac{w}{R}\right)\right]$$

$$N_{yB} = \frac{Et}{1-\nu^2}\left[\frac{\partial v}{\partial y} + \frac{w}{R} + \nu\left(\frac{\partial u}{\partial x} + \frac{d\bar{w}}{dx}\frac{\partial w}{\partial x}\right)\right]$$

Admissible expressions for u, v, and w, in keeping with the requirements of continuity around the cylinder are

$$u = U(x)\ \sin\frac{Jy}{R}$$

$$v = V(x)\ \cos\frac{Jy}{R} \qquad (12)$$

$$w = W(x)\ \sin\frac{Jy}{R}$$

where J is the number of peripheral waves around the cylinder. J must be a positive integer greater than 1. J = 1, represents a translation of the shell and J = 0 represents an axisymmetric form.

Substituting the expressions of (12) into Eqs. (11) we obtain the following set of equations:

$$\frac{d^2U}{dx^2} - \frac{1-\nu}{2}\frac{J^2}{R^2}U - \frac{(1+\nu)}{2}\frac{J}{R}\frac{dV}{dx} + \frac{\nu}{R}\frac{dW}{dx} + \frac{d}{dx}\left(\frac{d\bar{w}}{dx}\frac{dW}{dx}\right) - \frac{(1-\nu)}{2}\frac{J^2}{R^2}\frac{dw}{dx}W = 0$$

$$\frac{(1+\nu)}{2}\frac{J}{R}\frac{dU}{dx} - \frac{J^2}{R^2}V + \frac{1-\nu}{2}\frac{d^2V}{dx^2} + \frac{J}{R^2}W + \frac{(1-\nu)}{2}\frac{J}{R}\frac{d^2\bar{w}}{dx^2}W + \frac{(1+\nu)}{2}\frac{J}{R}\frac{d\bar{w}}{dx}\frac{dW}{dx} = 0 \qquad (13)$$

$$D\frac{d^4W}{dx^4} - 2\frac{DJ^2}{R^2}\frac{d^2w}{dx^2} + \frac{DJ^4}{R^4}W + \frac{1}{R}\overline{N_{yB}} + P\frac{d^2W}{dx^2} - \nu P\frac{J^2}{R^2}W + \frac{EtJ^2}{R^3}\bar{w}\,W\frac{d^2\bar{w}}{dx^2}\overline{N_{xB}} = 0$$

where

$$\overline{N_{xB}} = \frac{Et}{1-\nu^2}\left[\frac{dU}{dx} + \frac{d\bar{w}}{dx}\frac{dW}{dx} + \nu\left(\frac{-J}{R}V + \frac{W}{R}\right)\right]$$

$$\overline{N_{yB}} = \frac{Et}{1-\nu^2}\left[-\frac{J}{R}V + \frac{W}{R} + \nu\left(\frac{dU}{dx} + \frac{d\bar{w}}{dx}\frac{dW}{dx}\right)\right]$$

A solution for Eqs. (13) in this paper was obtained by means of the Galerkin method. The functions U(x),V(x), and W(x), appearing in the buckling displacements were expanded in sets of trigonometric functions, each set being selected so that each term of the buckling displacements satisfied completely the prescribed boundary conditions.

It was assumed that buckling is symmetrical about the center of the shell so that only one half of the shell needed to be analysed. The appropriate boundary conditions for the buckling displacements were then as follows:

$$\text{at} \qquad x = 0 \quad , \quad u = \frac{\partial v}{\partial x} = \frac{\partial w}{\partial x} = \frac{\partial^3 w}{\partial x^3} = 0$$

$$\text{at} \qquad x = \frac{L}{2} \quad , \quad u = v = w = \frac{\partial w}{\partial x} = 0$$

In order for these conditions to be fulfilled it was necessary, in view of the choice of expressions for the buckling displacements, that U, V, and W satisfy the following boundary conditions.

$$\text{at} \qquad x = 0 \quad , \quad U = \frac{dV}{dx} = \frac{dW}{dx} = \frac{d^3 W}{dx^3} = 0$$

$$\text{at} \qquad x = \frac{L}{2} \quad , \quad U = V = W = \frac{dW}{dx} = 0$$

Accordingly, the following expansions were chosen for U, V, and W.

$$U(x) = \sum_{n=1}^{k} u_n \sin \frac{n\pi x}{\ell}$$

$$V(x) = \sum_{n=1}^{k} v_n \cos \frac{(2n-1)\pi x}{2\ell} \qquad (14)$$

$$W(x) = \sum_{n=1}^{k} w_n \left[\cos \frac{(n-1)\pi x}{\ell} + \cos \frac{n\pi x}{\ell}\right]$$

Here u_n, v_n, w_n are unknown coefficients. When these expansions for U, V, and W are substituted into Eqs. (13), each of the three equations contains the 3k unknown coefficients, u_n, v_n, w_n. We now multiply each of the three equations by the appropriate trigonometric functions, one at a time, integrate over the interval $x = 0$, to $x = \ell$, and setting the result equal to zero (the Galerkin method), thereby obtain 3k linear homogeneous equations for the coefficients.

Finally, we must establish the lowest value of P, the loading per unit length along the edge of the shell, which will permit their coefficient matrix to have a zero determinant. It is this value of P which gives the load at which the shell will buckle. Since each choice of J, the number of peripheral waves around the shell, will have a buckling load associated with it we must investigate different values of J, to find the lowest of all possible buckling loads.

In presenting the matrix at hand, that is the matrix of the coefficients u_n, v_n and w_n, denoted herein as matrix A, it is advantageous at this time to introduce some abbreviations. In addition to employing the Kroniker delta, denoted by the symbol δ, the following notation is also used

$$\int_0^{\ell} \cosh a_1x \cos a_2x \sin a_3x \sin a_4x \, dx =$$

$$= \text{CCSS } a_1, a_2, a_3, a_4$$

The first large capital always refers to a hyperbolic function, either C denoting cosh or S denoting sinh. The following three letters represent the trigonometric functions, C denoting cosine and S denoting sine, and the following four lower case letters represent quantities appearing as shown above.

Carrying out the integration procedure described earlier, we then obtain for the elements of the matrix A, for

$$0 < n \leq K$$

$$0 < m \leq K$$

$$A_{m,n} = \frac{\ell}{2} \left\{ \frac{(\nu-1)\ J^2}{2\ R^2} - \frac{(n\pi)^2}{\ell^2} \right\} \delta_{m,n}$$

for

$$K < n \leq 2K$$

$$0 < m \leq K$$

$$A_{m,n} = \frac{(1+\nu)(2n-1)J}{4R} \left\{ \frac{\sin(2n-1-2m)\ \pi/2}{(2n-1-2m)} - \frac{\sin(2n-1+2m)\ \pi/2}{(2n-1+2m)} \right\}$$

for

$$2K < n \leq 3K$$

$$0 < m \leq K$$

$$A_{m,n} = \frac{(1-n)\pi\nu}{2R} \delta_{m,n-1}$$

$$- \frac{\nu n\pi}{2R} \delta_{m,n}$$

$$- \gamma_1 \left[\left(\frac{(n-1)\ \pi}{\ell} \right)^2 + \frac{(1-\nu)\ J^2}{2R^2} \right] \text{CSCS } \phi,\ \theta,\ \left\{ \frac{(n-1)\ \pi}{\ell} \right\},\ \left\{ \frac{m\pi}{\ell} \right\}$$

$$- \gamma_2 \left[\left(\frac{(n-1)\ \pi}{\ell} \right)^2 + \frac{(1-\nu)\ J^2}{2R^2} \right] \text{SCCS } \phi,\ \theta,\ \left\{ \frac{(n-1)\ \pi}{\ell},\ \frac{m\pi}{\ell} \right\}$$

$$- \gamma_1 \left[\left(\frac{n\pi}{\ell}\right)^2 + \frac{(1-\nu)\ J^2}{2R^2} \right] \ \mathrm{CSCS}\ \phi,\ \theta,\ \{\frac{n\pi}{\ell}\},\ \{\frac{m\pi}{\ell}\}$$

$$- \gamma_2 \left[\left(\frac{n\pi}{\ell}\right)^2 + \frac{(1-\nu)\ J^2}{2R^2} \right] \ \mathrm{SCCS}\ \phi,\ \theta,\ \{\frac{n\pi}{\ell}\},\ \{\frac{m\pi}{\ell}\}$$

$$+ \frac{(1-n)\ \gamma_3 \pi}{\ell} \ \mathrm{SSSS}\ \phi,\ \theta,\ \{\frac{(n-1)\ \pi}{\ell}\},\ \{\frac{m\pi}{\ell}\}$$

$$+ \frac{(1-n)\ \gamma_4 \pi}{\ell} \ \mathrm{CCSS}\ \phi,\ \theta,\ \{\frac{(n-1)\ \pi}{\ell}\},\ \{\frac{m\pi}{\ell}\}$$

$$- \frac{n\pi\gamma_3}{\ell} \ \mathrm{SSSS}\ \phi,\ \theta,\ \{\frac{n\pi}{\ell}\},\ \{\frac{m\pi}{\ell}\}$$

$$- \frac{n\pi\gamma_4}{\ell} \ \mathrm{CCSS}\ \phi,\ \theta,\ \{\frac{n\pi}{\ell}\},\ \{\frac{m\pi}{\ell}\}$$

for

$$0 < n \leq K$$

$$K < m \leq 2K$$

$$A_{m,n} = \frac{(1+\nu)\ Jn}{2R} \left\{ \frac{\sin(n-m+1/2)\pi}{(2n-2m+1)} + \frac{\sin(n+m-1/2)\pi}{(2n+2m-1)} \right\}$$

for

$$K < n \leq 2K$$

$$K < m \leq 2K$$

$$A_{m,n} = \frac{\ell}{2} \left\{ \frac{-J^2}{R^2} - \frac{(1-\nu)(2n-1)^2\pi^2}{8\ell^2} \right\} \ \delta_{m,n}$$

for $2K < n \leq 3K$

$K < m \leq 2K$

$$A_{m,n} = \frac{J\ell}{R^2\pi} \left\{ \frac{\sin\ (2n-2m-1)\ \pi/2}{(2n-2m-1)} + \frac{\sin\ (2n+2m-3)\ \pi/2}{(2n+2m-3)} \right\}$$

$$+ \frac{J\ell}{\pi R^2} \left\{ \frac{\sin\ (n-m+1/2)\ \pi}{(2n-2m+1)} + \frac{\sin\ (n+m-1/2)\pi}{(2n+2m-1)} \right\}$$

$$+ \left\{ \frac{(1-\nu)}{2} \frac{J}{R} \gamma_3 \right\} \text{ SSCC } \phi,\ \theta,\ \left\{ \frac{(n-1)\pi}{\ell} \right\}, \left\{ \frac{(2m-1)\ \pi}{2\ell} \right\}$$

$$+ \frac{(1-\nu)}{2} \frac{J}{R} \gamma_3 \quad \text{SSCC } \phi,\ \theta,\ \left\{ \frac{n\pi}{\ell} \right\},\ \left\{ \frac{(2m-1)\ \pi}{2\ell} \right\}$$

$$+ \left\{ \frac{(1-\nu)}{2} \frac{J}{R} \gamma_4 \quad \text{CCCC } \phi,\ \theta,\ \left\{ \frac{(n-1)\ \pi}{\ell} \right\},\ \left\{ \frac{(2m-1)\ \pi}{2\ell} \right\} \right.$$

$$+ \left\{ \frac{(1-\nu)\ J\ \gamma_4}{2R} \right\} \text{ CCCC } \phi,\ \theta,\ \left\{ \frac{n\pi}{\ell} \right\},\ \left\{ \frac{(2m-1)\ \pi}{2\ell} \right\}$$

$$+ \frac{(1+\nu)\ J\ (1-n)\pi\gamma_1}{2R\ell} \text{ CSSC } \phi,\ \theta,\ \left\{ \frac{(n-1)\ \pi}{\ell} \right\},\ \left\{ \frac{(2m-1)\ \pi}{2\ell} \right\}$$

$$+ \frac{(1+\nu)\ J\ (1-n)\pi\gamma_2}{2R\ell} \text{ SCSC } \phi,\ \theta,\ \left\{ \frac{(n-1)\pi}{\ell} \right\},\ \left\{ \frac{(2m-1)\ \pi}{2\ell} \right\}$$

$$- \frac{(1+\nu)\ J\ n\pi\gamma_1}{2R\ell} \quad \text{CSSC } \phi,\ \theta,\ \left\{ \frac{n\pi}{\ell} \right\},\ \left\{ \frac{(2m-1)\ \pi}{2\ell} \right\}$$

$$- \frac{(1+\nu)\ J\ n\pi\gamma_2}{2R\ell} \text{ SCSC } \phi,\ \theta,\ \left\{ \frac{n\pi}{\ell} \right\},\ \left\{ \frac{(2m-1)\ \pi}{2\ell} \right\}$$

for $$0 < n \leq K$$

$$2K < m \leq 3K$$

$$A_{m,n} = \frac{\nu ET\ n\ \pi}{2R(1-\nu^2)} \qquad \delta_{m,n}$$

$$+ \frac{\nu ET\ n\ \pi}{2R(1-\nu^2)} \qquad \delta_{(m-1),n}$$

$$- \frac{ETn\pi\gamma_3}{\ell(1-\nu^2)} \{SSCC\ \phi,\ \theta,\ \{\frac{n\pi}{\ell}\}\ ,\ \{\frac{(m-1)\ \pi}{\ell}\} + SSCC\ \phi,\ \theta,\ \{\frac{n\pi}{\ell}\},\ \{\frac{m\pi}{\ell}\}\}$$

$$- \frac{ETn\pi\gamma_4}{\ell(1-\nu^2)}\ \{CCCC\ \phi,\ \theta,\ \{\frac{n\pi}{\ell}\}\ ,\ \{\frac{(m-1\ \pi}{\ell}\} + CCCC\ \phi,\ \theta,\ \{\frac{n\pi}{\ell}\}\ ,\ \{\frac{m\pi}{\ell}\}\}$$

for $$K < n \leq 2K$$

$$2K < m \leq 3K$$

$$A_{m,n} = \frac{-ETJ\ \ell}{\pi R^2(1-\nu^2)} \{\frac{\sin(2m-2n-1)\ \pi/2}{(2m-2n-1)} + \frac{\sin(2m+2n-3)\ \pi/2}{(2m+2n-3)}$$

$$+ \frac{\sin\ \pi(m-n+1/2)}{(2m-2n+1)} + \frac{\sin\ \pi(m+n-1/2)}{(2m+2n-1)}\}$$

$$+ \frac{ET\nu J\gamma_3}{R(1-\nu^2)}\ \{SSCC\phi,\theta,\{\frac{(2n-1)\pi}{2\ell}\},\{\frac{(m-1)\pi}{\ell}\}+SSCC\phi,\theta,\{\frac{(2n-1)\pi}{2\ell}\},\{\frac{m\pi}{\ell}\}\}$$

$$+ \frac{ET\nu J\gamma_4}{R(1-\nu^2)}\ \{CCCC\phi,\theta,\ \{\frac{(2n-1)\pi}{2\ell}\},\{\frac{(m-1)\pi}{\ell}\}+CCCC\phi,\theta,\ \{\frac{(2n-1)\pi}{2\ell}\}\ ,\{\frac{m\pi}{\ell}\}\}$$

for

$$2K < n \leq 3K$$

$$2K < m \leq 3K$$

$$A_{mn} = \Big\{ D\left(\frac{(n-1)\pi}{\ell}\right)^4 \frac{\ell}{2} + D\left(\frac{n\pi}{\ell}\right)^4 \frac{\ell}{2} + \frac{J^2D\ (n-1)^2\pi^2}{R^2\ell}$$

$$+ \frac{J^2D\ n^2\pi^2}{R^2\ell} + \frac{Et\ell}{(1-\nu^2)R^2} + \frac{D\ell J^4}{R^4} - \frac{P(n-1)^2\pi^2}{2\ell}$$

$$- \frac{Pn^2\pi^2}{2\ell} \Big\} \quad \delta_{m,n}$$

$$+ \{\frac{D(n-1)^4\pi^4}{2\ell^3} + \frac{DJ^2(n-1)^2\pi^2}{R^2\ell} + \frac{ET\ell}{2R^2(1-\nu^2)} + \frac{D\ell J^4}{2R^4}$$

$$- \frac{P(n-1)^2\pi^2}{2\ell} + \frac{EtJ^2q\ell}{2R^3} - \frac{\nu PJ^2\ell}{2R^2}\} \quad \delta_{m,n-1}$$

$$+ \{\frac{Dn^4\pi^4}{2\ell^3} + \frac{DJ^2n^2\pi^2}{R^2\ell} + \frac{ET\ell}{2R^2(1-\nu^2)} + \frac{D\ell J^4}{2R^4} - \frac{Pn^2\pi^2}{2\ell}$$

$$+ \frac{ETJ^2q\ell}{2R^3} - \frac{\nu PJ^2\ell}{2R^2}\} \quad \delta_{m,\ n+1}$$

$$- \frac{\nu ET\gamma_1 (n-1)\pi}{R\ell(1-\nu^2)} \{CSSC\phi,\theta,\ \{\frac{(n-1)\pi}{\ell}\}\ ,\ \{\frac{(m-1)\pi}{\ell}\} + CSSC\phi,\theta,\ \{\frac{(n-1)\pi}{\ell}\},\ \{\frac{m\pi}{\ell}\}\}$$

$$- \frac{\nu ET\gamma_1 n\ \pi}{R\ell(1-\nu^2)} \{CSSC\phi,\theta,\ \{\frac{n\pi}{\ell}\}\ ,\ \{\frac{(m-1)\pi}{\ell}\} + CSSC\phi,\theta,\ \{\frac{n\pi}{\ell}\}\ ,\ \{\frac{m\pi}{\ell}\}\}$$

$$- \frac{\nu ET\gamma_2 (n-1)\pi}{R\ell(1-\nu^2)} \{SCSC\phi,\theta,\ \{\frac{(n-1)\pi}{\ell}\},\ \{\frac{(m-1)\pi}{\ell}\} + SCSC\phi,\theta,\ \{\frac{(n-1)\pi}{\ell}\}\ ,\ \{\frac{m\pi}{\ell}\}\}$$

$$- \frac{\nu ET\gamma_2 n\pi}{R\ (1-\nu^2)\ell} \{SCSC,\phi,\theta,\ \{\frac{n\pi}{\ell}\}\ ,\ \{\frac{(m-1)\pi}{\ell}\} + SCSC\phi,\theta,\ \{\frac{n\pi}{\ell}\}\ ,\ \{\frac{m\pi}{\ell}\}\}$$

$$+ \frac{ETJ^2C_1}{R^3} \{SSCC\phi,\theta,\ \{\frac{(n-1)\pi}{\ell}\}\ ,\ \{\frac{(m-1)\pi}{\ell}\} + SSCC\phi,\theta,\ \{\frac{(n-1)\pi}{\ell}\}\ ,\ \{\frac{m\pi}{\ell}\}$$

$$+ SSCC\phi,\theta,\ \{\frac{n\pi}{\ell}\}\ ,\ \{\frac{(m-1)\pi}{\ell}\} + SSCC\phi,\theta,\ \{\frac{n\pi}{\ell}\}\ ,\ \{\frac{m\pi}{\ell}\}\}$$

$$+ \frac{ETJ^2C_2}{R^3} \{CCCC,\phi,\theta,\ \{\frac{(n-1)\pi}{\ell}\}\ ,\ \{\frac{(m-1)\pi}{\ell}\}\ + CCCC\phi,\theta,\ \{\frac{(n-1)\pi}{\ell}\}\ ,\ \{\frac{m\pi}{\ell}\}$$

$$+ CCCC\phi,\theta,\ \{\frac{n\pi}{\ell}\}\ ,\ \{\frac{(m-1)\pi}{\ell}\} + CCCC\phi,\theta,\ \{\frac{n\pi}{\ell}\}\ ,\ \{\frac{m\pi}{\ell}\}\}$$

$$- \frac{\nu ET\gamma_3}{R(1-\nu^2)} \{SSCC\phi,\theta,\ \frac{(n-1)\pi}{\ell}\ ,\ \frac{(m-1)\pi}{\ell} + SSCC\phi,\theta,\ \frac{(n-1)\pi}{\ell}\ ,\ \frac{m\pi}{\ell}$$

$$+ SSCC\ \phi,\theta,\ \{\frac{n\pi}{\ell}\}\ ,\ \{\frac{(m-1)\pi}{\ell}\} + SSCC\ \phi,\theta\ ,\ \{\frac{n\pi}{\ell}\},\ \{\frac{m\pi}{\ell}\}\}$$

$$- \frac{\nu E T \gamma_4}{R(1-\nu^2)} \{CCCC\phi,\theta, \frac{(n-1)\pi}{\ell} , \frac{(m-1)\pi}{\ell} + CCCC\ \phi,\theta, \frac{(n-1)\pi}{\ell} , \frac{m\pi}{\ell}$$

$$+ CCCC\phi,\theta, \frac{n\pi}{\ell} , \frac{(m-1)\pi}{\ell} + CCCC\ \phi,\theta, \frac{n\pi}{\ell} , \frac{m\pi}{\ell}\}$$

$$+ \frac{E T \gamma_1 \gamma_3 (n-1)\pi}{4\ell(1-\nu^2)} \{SCSC\ 2\phi,0, \frac{(n-1)\pi}{\ell} , \frac{(m-1)\pi}{\ell} + SCSC\ 2\phi,\ 0, \frac{(n-1)\pi}{\ell} , \frac{m\pi}{\ell}$$

$$- SCSC\ 2\phi,2\theta, \frac{(n-1)\pi}{\ell} , \frac{(m-1)\pi}{\ell} - SCSC\ 2\phi,\ 2\theta, \frac{(n-1)\pi}{\ell} , \frac{m\pi}{\ell}\}$$

$$- \frac{E T \gamma_1 \gamma_3 n\pi}{4\ell(1-\nu^2)} \{SCSC\ 2\phi,\ 2\theta, \frac{n\pi}{\ell} , \frac{(m-1)\pi}{\ell} + SCSC\ 2\phi,\ 2\theta, \frac{n\pi}{\ell} , \frac{m\pi}{\ell}$$

$$- SCSC\ 2\phi,\ 0, \frac{n\pi}{\ell} , \frac{(m-1)\pi}{\ell} - SCSC\ 2\phi,\ 0, \frac{n\pi}{\ell} , \frac{m\pi}{\ell}\}$$

$$+ \frac{E T \gamma_2 \gamma_3 (n-1)\pi}{4\ell(1-\nu^2)} \{CSSC\ 2\phi,\ 2\theta, \frac{(n-1)\pi}{\ell} , \frac{(m-1)\pi}{\ell} + CSSC\ 2\phi,\ 2\theta, \frac{(n-1)\pi}{\ell} , \frac{m\pi}{\ell}$$

$$- CSSC\ 0,\ 2\theta, \frac{(n-1)\pi}{\ell} , \frac{(m-1)\pi}{\ell} - CSSC\ 0,\ 2\theta, \frac{(n-1)\pi}{\ell} , \frac{m\pi}{\ell}\}$$

$$+ \frac{E T \gamma_2 \gamma_3 n\pi}{4\ell(1-\nu^2)} \{CSSC\ 2\phi,\ 2\theta, \frac{n\pi}{\ell} , \frac{(m-1)\pi}{\ell} + CSSC\ 2\phi,\ 2\theta, \frac{n\pi}{\ell} , \frac{m\pi}{\ell}$$

$$- CSSC\ 0,\ 2\theta, \frac{n\pi}{\ell} , \frac{(m-1)\pi}{\ell} - CSSC\ 0,\ 2\theta, \frac{n\pi}{\ell} , \frac{m\pi}{\ell}\}$$

$$+\frac{ET\gamma_1\gamma_4(n-1)\pi}{4\ell(1-\nu^2)}\{CSSC\ 2\phi,\ 2\theta,\ \frac{(n-1)\pi}{\ell},\ \frac{(m-1)\pi}{\ell} + CSSC\ 2\phi,\ 2\theta,\ \frac{(n-1)\pi}{\ell},\ \frac{m\pi}{\ell}$$

$$+ CSSC\ 0,\ 2\theta,\ \frac{(n-1)\pi}{\ell},\ \frac{(m-1)\pi}{\ell} + CSSC\ 0,\ 2\theta,\ \frac{(n-1)\pi}{\ell},\ \frac{m\pi}{\ell}\}$$

$$+\frac{ET\gamma_1\gamma_4 n\pi}{4\ell(1-\nu^2)}\{CSSC\ 2\phi,\ 2\theta,\ \frac{n\pi}{\ell},\ \frac{(m-1)\pi}{\ell} + CSSC\ 2\phi,\ 2\theta,\ \frac{n\pi}{\ell},\ \frac{m\pi}{\ell}$$

$$+ CSSC\ 0,\ 2\theta,\ \frac{n\pi}{\ell},\ \frac{(m-1)\pi}{\ell} + CSSC\ 0,\ 2\theta,\ \frac{n\pi}{\ell},\ \frac{m\pi}{\ell}\}$$

$$+\frac{ET\gamma_2\gamma_4(n-1)\pi}{4\ell(1-\nu^2)}\{SCSC\ 2\phi,\ 0,\ \frac{(n-1)\pi}{\ell},\ \frac{(m-1)\pi}{\ell} + SCSC\ 2\phi,\ 0,\ \frac{(n-1)\pi}{\ell},\ \frac{m\pi}{\ell}$$

$$+ SCSC\ 2\phi,\ 2\theta,\ \frac{(n-1)\pi}{\ell},\ \frac{(m-1)\pi}{\ell} + SCSC\ 2\phi,\ 2\theta,\ \frac{(n-1)\pi}{\ell},\ \frac{m\pi}{\ell}\}$$

$$+\frac{ET\gamma_2\gamma_4 n\pi}{4\ell(1-\nu^2)}\{SCSC\ 2\phi,\ 0,\ \frac{n\pi}{\ell},\ \frac{(m-1)\pi}{\ell} + SCSC\ 2\phi,\ 0,\ \frac{n\pi}{\ell},\ \frac{m\pi}{\ell}$$

$$+ SCSC\ 2\phi,\ 2\theta,\ \frac{n\pi}{\ell},\ \frac{(m-1)\pi}{\ell} + SCSC\ 2\phi,\ 2\theta,\ \frac{n\pi}{\ell},\ \frac{m\pi}{\ell}\}$$

Experimental Procedure

Specimen Preparation

Thin-walled cylindrical shells were fabricated from an eppoxy resin and hardener compound using the centrifugal casting technique. This technique was first discussed in Ref. [11]. The casting facility consisted of an acrylic drum which rotated on a horizontal axis and is shown in Fig. 4. The drum was carefully machined and fitted with close fitting end plates which, in turn, were mounted on brass hubs. A specially selected 1 1/4" dia. ground and hardened steel shaft was passed through these hubs. The shaft was supported at each end by high precision ball bearings located on heavy pedestals. The pedestals were fastened to a concrete base. The assembly was driven by V belt from a 1/2 H.P. variable speed electric drive.

The acrylic drum had inner dimensions of 18" in length and 8" in diameter. The wall was 1/2" thick and the end plates 3/4" thick. Six 250 watt infra-red lamps were used to provide heat and promote curing of the eppoxy. The drum was rotated at 1200 RPM during shell curing and it was found to be virtually free of vibration effecting forming of the shells.

In the preparation of a thin cylindrical shell a certain sequence of steps was carried out. These steps are described in order as follows:

(1) Wipe the inner drum surface with mold release, (Hysol Co. No. AC4-4367 was used.)

(2) Spin the drum with heat lamps turned on to dry the mold release and heat up the drum.

(3) Cast a shell liner in the drum. This is accomplished by mixing the appropriate amount of Hysol Co. Resin No. R8-2038 with Hysol Hardener No. H2-3404 in proper proportions (100 to 11, Resin to Hardener, by weight) and pouring it into the drum through holes in the end plates. The drum is then rotated for about 3 hours with the heat lamps turned on while the liner hardens. The object of the liner is to remove the effect of any small irregularities that might exist on the inner drum surface. The inner surface of the hardened liner now controls the outer surface of the shell to be cast.

(4) Wipe the inner liner surface with mold release and once again rotate the drum with lamps on to dry the mold release.

(5) Mix the necessary amount of Resin and hardener to provide the required shell thickness and add it to the drum. Rotate the drum, with lamps on, for about 10 hours to completely cure the shell.

(6) Remove the cured shell. This is accomplished by pushing the shell and liner assembly out through one end of the disassembled drum. The liner is then cut free of the shell. The shell is wiped off with trichloroethane and is ready for testing.

The shells produced in the above manner have a number of features which are highly desirable for the purpose of testing. These features may be listed as follows:

(1) Shell geometry is extremely good. Shells produced in this manner, with thicknesses of 0.020 in., 0.025 in. and 0.030 in., were found to have a thickness variation of not more than 0.0005 in. Furthermore, cylindrical shells of various geometry can be readily produced. Since the length and

diameter are determined by those of the drum, almost any dimensions can be achieved by varying drum geometry. Thickness of shell walls is controlled by selecting the proper amount of liquid resin and hardener.

(2) The customary problem of effecting a proper bond at shell wall seams is eliminated since there are no seams.

(3) In view of the method of shell production there are no residual stresses in the walls and no initial deformations.

(4) Given sufficient time between tests (approximately 2 hours) the material of the shells undergoes complete elastic recovery from buckling deformations and they may be (and have been) tested over and over again with the same buckling loads reached in successive tests.

(5) An important additional feature of these shells is the fact that the material from which they are made is translucent and bi-refringent. A photoelastic analysis of the prebuckling, buckling and postbuckling strains of the shells is thus made possible. The reflective (photostress) technique has been used to study the strains.

Still, and high speed photography have both been used to study the strain distributions. A Budd Co. L.F.Z. large field meter has been employed in all photoelastic studies.

Testing Apparatus

Shells were tested in a 4 screw Tinnius Olsen Universal Testing Machine (Fig. 5). Shell end plates were fabricated from 3/4" thick, 10" outer diameter circular steel plates. These plates were ground on both sides. A 1/2" wide, 5/16" deep, concentric circular groove was first machined in each plate. Next a 3/32" wide, 1/16" deep, circular groove, with outer diameter matching that of the shell was recessed in the center of the first groove. In addition each end plate was fitted with an O-ring seal, while one plate was fitted with a pneumatic fitting, so that pressure or vacuum could be applied to the shell as required.

In preparing a shell for testing the following steps were carried out.

(1) The inner surface was spray painted with reflective aluminum paint. This step was required so that a photoelastic study of the strains could be carried out using the photostress technique. The difficulty encountered in trying to achieve a thin uniform deposit of paint on the surface was overcome with the aid of a small blower. The blower was used to maintain an air stream flowing through the shell. An aluminum spray can was used to maintain a fog of paint in the air stream, the paint being gradually deposited on the shell surface. In this manner a very satisfactory reflective surface was achieved.

(2) One end plate was placed on a level table with the grooved side up. The shell to be tested was then positioned in the groove. Hysol Resin and hardener, mixed as described above, was poured into the groove. Three equally spaced holes of 1/4" diameter which had been drilled into the inner groove allowed the mixture to flow across beneath the shell so that the inner groove and outer groove were each filled up to the level of the upper plate surface. The assembly was then left to cure for about 8 hours. Following the curing the shell was rigidly imbedded in the end plate.

(3) The assembly was then placed in the testing machine and the end plate was fastened with cap screws to the levelling plate (see Fig. 5) which in turn was "spring loaded" against the upper platten of the machine. The end plate for the lower end of the shell was then placed in position on the lower platten and the upper platten was lowered until the shell bottom end entered into the groove of the end plate. The lower groove was then filled with Resin and hardener and left for 8 hours to cure. The shell, which then had rigidly built-in ends, was virtually free of initial stresses at the edge. Now the shell was ready for testing.

<u>Testing Procedure</u>

In order to insure that the end plates of the shell remained parallel during testing, a levelling plate was used (see Fig. 5). This plate had 3 levelling screws, threaded through it and resting against the upper platten. The screws were equally spaced on a circle of 11 1/2" diameter. A dial gage was mounted beside each screw in such a way that it indicated changes in distance between the end plates at that point. Initially all dial gages were set to zero. During the testing process the loading was periodically interrupted so that the gage readings could be compared and the levelling screws adjusted as required. In this way parallelism of end plates could be controlled so that the dial gage readings did not differ by more than 0.0005" at buckling.

The loading was also interrupted as required so that photographs of the shell could be taken through the photostress field meter. A 1" x 1" grid, which was traced on the shell outer surface with a grease pencil, made possible the establishment of physical locations of fringe orders and isoclinic lines, etc., observed in these photographs.

Photoelastic Study

Prebuckling Deformations

It is known from the theory of photoelasticity that fringe orders obtained at any point, when conducting isochromatic studies, vary linearly with the maximum shear stress resultant at the point. Using Eqs. (3)b and (4) to express N_y in terms of displacements we have

$$N_y = \frac{Et}{(1-\nu^2)} \left[\frac{w}{R} + \nu \left(\frac{du}{dx} + \frac{1}{2} \left(\frac{dw}{dx}\right)^2\right)\right] \tag{15}$$

Substituting for du/dx from (5) we obtain

$$N_y = \frac{Et}{(1-\nu^2)} \left[(1-\nu^2) \frac{w}{R} - (1-\nu^2) \frac{\nu P}{Et}\right] \tag{16}$$

therefore

$$N_y = Et \frac{w}{R} - \nu P \tag{17}$$

In view of the fact that N_x and N_y are the principal stresses at any point of the prebuckled shell, the maximum shear stress resultant at any point is given by

$$\frac{N_x - N_y}{2t} = \frac{1}{2t} \left[P(\nu-1) - \frac{Etw}{R}\right] \tag{18}$$

In fig. 6 the ratio of maximum shear stress resultant to maximum shear stress resultant with edge effects neglected is plotted for a cylindrical shell subjected to a load equal to 90% of the Euler buckling load. Figure 7 is a view of the corresponding isochromatics. These isochromatics are shown in color in Fig.

8a. An interesting and informative study of the agreement between experimental and analytical results is thus made possible. Studies indicate good agreement between theoretical and experimental radial deflections.

The rapid variation in maximum shear stress resultant, predicted by theory and manifested by this succession of rings, is due to the rapid variation in tangential (hoop) stress along the shell. The tangential stress variation, in turn, is due to the rapid variation in radial displacement caused by the clamped condition at the shell edges. Since the radial displacement along the shell is almost of the damped sinusoidal type, the tangential stress variation is rapidly damped out on moving in from the edge of the shell.

It is the existence of these nonuniform stresses and displacements, observed in this photoelastic study, that makes the membrane stress model used in classical linear theory inadequate for describing the actual cylindrical shell at the incipience of buckling. In a correct analysis of buckling behavior the influence of these stresses and deformations must be taken into consideration.

Post Buckled Configurations

In almost every test conducted under axial load and without internal pressure the shell buckled into a two tier, six peripheral wave, diamond shape configuration. Photographs of the 90° isoclinics and the isochromatics for a typical shell are shown in Figs. 8b, c. These buckles were located almost midway ($\pm$ 1/4") along the shell. The exact periodicity of the buckles, around the shell, as well as the symmetry observed in the photographs attest to the caution used in fabricating and testing. With internal pressure the number of buckles around the shell increased and the tiers tended to move toward one of the edges.

Discussion and Conclusions

Analytical Results

(a) Computed Buckling Loads

The analytical computations were carried out on an IBM 7074 digital computer. The print-out of a typical program (Fort-Pitt) is contained in Appendix I. In order to maximize the size of matrices which this computer could handle, the matricies were computed and stored, one section at a time, on a storage tape. Next, with the matrix generating program not required, and having more storage space available in the computer, the determinants of the matrices were evaluated. This largest matrix corresponded to a 24 term expansion of the displacement functions. All the analytical results reported herein are based on a 24 term expansion unless stated otherwise.

In order to conserve computer time the usual custom was to first take a "fast pass" at finding the approximate buckling load. This was done using a 12 term expansion and letting P* vary from approximately 0.05 to 1.0 in intervals of 0.05. The buckling load to be predicted was known to be in the neighborhood of the first crossing of the axis (change in sign of the determinant). The next step was to increase the number of expansion terms to the desired level ≤ 24, and investigate the location of the lowest zero using finer increments.

Examining Eq. (8) we note that the quantity θ, which determines the wavelength of the trigonometric functions appearing in the prebuckling radial displacements, is independent of shell length. It is therefore to be expected that a proper analysis pertaining to shells of greater length, and hence more prebuckling waves, will require the use of more terms in the trigonometric expansions and hence larger matrices. The first analysis was therefore carried out on a shell with ratio of length to radius (L/R) equal to 0.75. This was the shortest length of shell investigated.

In Fig. 9 the buckling load P* vs. J, the number of peripheral waves, is presented for this shell, based on a 12 term expansion. We note that the load reaches a minimum for J = 10. In Fig. 10 the computed buckling load vs. internal pressure parameter is given for the same shell, with J chosen to minimize the load, and number of terms K, equal to 24.

Analytical results for different shell geometries, with J = 2, are presented in Figs. 13, 14, 15, and 16. In all cases the buckling loads were found to undergo small increases with pressure at first and then level off and become independent of pressure. In Fig. 17 analytical results are given for an unpressurized shell. Here we note the significant improvement in agreement between experimental and analysis as we increase the number of terms in the expansions from 12 to 24.

(b) <u>Effects of Number of Terms used in Trigonometric Expansions</u>

This investigation was concerned with an unpressurized shell with ratio of length to radius (L/R) = 3. Here it was found that the effect of varying J was much more critical (see Fig. 11). Buckling loads have been computed using 8, 12, and 24 term expansions. It is noted that for J = 2 and J = 4 the values of the predicted buckling loads are equal and sensitivity to the number of terms appears to be nil for K > 12.

At J = 6 the results become more sensitive to the number of terms and for J = 8, up to 10, the buckling loads, based on a 24 term expansion, begin to drop quite sharply. At J = 12, the load begins to increase again, having reached a minimum at J = 10. In Fig. 12 the buckling load vs. internal pressure parameter is plotted for this shell with values of J = 2 and J = 8. We note that the load increases rapidly with pressure for J = 8, and eventually begins to level off at a loading slightly above that obtained for J = 2. This indicates that the discrepancy between analysis and experiment for longer shells with higher values of J is centered around the region of zero and low internal pressures only.

On studying the equilibrium equations (Eqs. 13) we note that the parameter J appears in the first two equations in powers not greater than the second. In the third equation the maximum power to which it appears is the fourth. This means that some components which go into making up the matrix elements associated with the third equation will change by a factor of 10,000/16, as J changes from 2 to 10. This extreme change brought about by alteration of J may have a highly significant effect on the number of terms required for proper computation, in particular for longer shells.

A more thorough investigation of the effect of the number of terms on the outcome of such computations is given in Appendix 1.

Experimental Results

(a) Experimental Buckling Loads

Shells with ratios of radius to thickness (R/t) ranging from 133 to 200 were tested. The lengths varied from 0.75 to 4.3 radii, the radius in each case being equal to 4 inches.

Experimental buckling loads vs. internal pressure parameter, are presented for various shell geometries in Fig. 10, and Fig. 13 through 18. In all experiments the buckling loads initially increased with internal pressure to about 10% above that of the unpressurized shell. The loads then levelled off and were no longer appreciably effected by increased pressure.

(b) Effects of Shell Length and Ratio of Radius to Thickness

In Fig. 22, the buckling load vs. ratio of length to radius for an unpressurized shell of fixed thickness and radius is presented. The buckling load was found to be almost independent of length for $L/R \geq 1.5$. It drops off by about 4% as L/R decreases to .75. The loads were found not to be appreciably affected by changes in R/t within the range of geometrics investigated.

Comparison of Analytical and Experimental Results

In figure 10 the analytical and experimental results are presented for a pressurized shell with ratio of length to radius equal to 0.75. The computed and experimental buckling loads for the unpressurized shell agree to within about 2 1/2%. For the internally pressurized shell the experimental and analytically predicted buckling loads both rise with pressure, however, the loads predicted by analysis rise somewhat faster at first. Both curves level out eventually and are no longer effected by pressure.

The analytical and experimental results for a longer unpressurized shell (L/R=3.0) with different values of J used in the analysis are presented in Fig. 11. Here we note that for values of J from 2 up to 6 we have good agreement between experiment and analysis. For values of J from 7 up to 10 the experiment and analysis begin to differ quite rapidly, with the disagreement being a maximum at J=10. For J greater than 10 the analytical results begin to move up again toward those of experiment. The cause of this disagreement was discussed earlier.

Comparison of experimental and analytical results for pressurized shells of various geometrics is presented in figures 13, 14, 15, and 16. The analysis is restricted here to the case of J=2. It is noted that the agreement between experiment and analysis is good for zero pressure. While both analytic and experimental buckling loads increase with internal pressure, the increase encountered in experiment is considerably greater than that for the analysis. In both cases the loads level off at higher pressures.

Conclusions

The effect of nonuniform prebuckling deformations brought about by edge supports, in reducing the buckling loads of clamped thin-walled cylinders subjected to axial and lateral loading, is confirmed by both the experimental and analytical results reported herein.

Reductions from the Euler buckling loads of not more than 15% have been encountered. It is, therefore, apparent that an explanation for the much larger discrepencies more commonly encountered in shell testing will have to be found in the effects of imperfections in the specimens as well as techniques used for supporting of the edges and application of loading.

A study of the governing equations and the analytical results indicates that larger matrices are required for investigating the buckling loads of longer shells ($L/R>1.0$), in particular where low interval pressures are involved.

It should be pointed out at this time that while the analysis carried out pertains to shells with clamped edges, shells with many other types of edge conditions may be analysed provided that appropriate sets of functions are chosen for expansion of the buckling displacements.

The inadequacy of the classical membrane model to describe the shell in the prebuckling regime has already been discussed. Its inadequacy for describing the shell at buckling is born out by both the experimental and analytical results. The effects of large non-uniform prebuckling deformations must be incorporated into any analysis of the buckling of thin-wall shells subjected to combinations of axial loading and internal pressure.

The isolation of the effects of these deformations has been made possible through the preparation of test specimens which are virtually free of imperfections as well as the high degree of accuracy used in fitting edge supports. The caution used in the application of loading has also been a contributing factor.

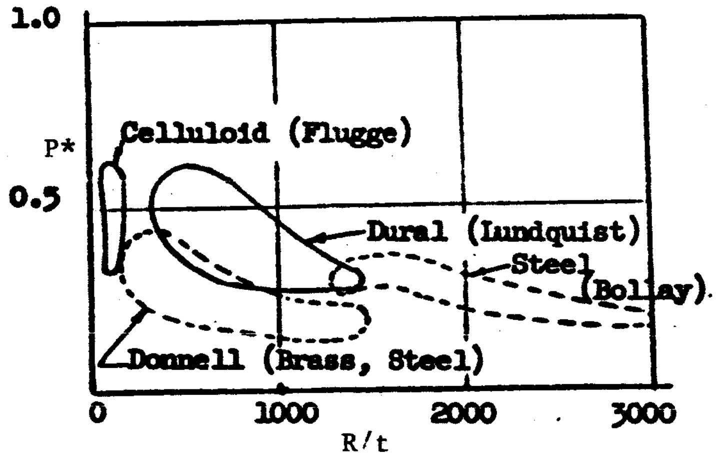

Fig. I. Regions Containing Experimental Points Obtained by Various Experimenters.

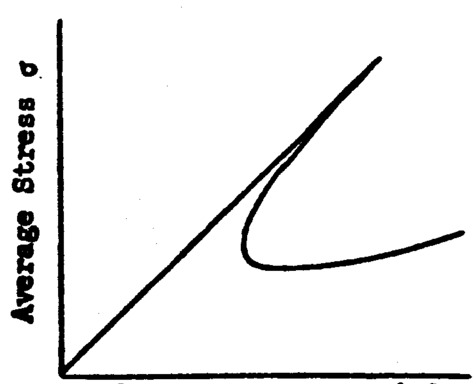

Fig. II. Average Stress vs. Cylinder Shortening as Computed by Von Karman and Tsien.

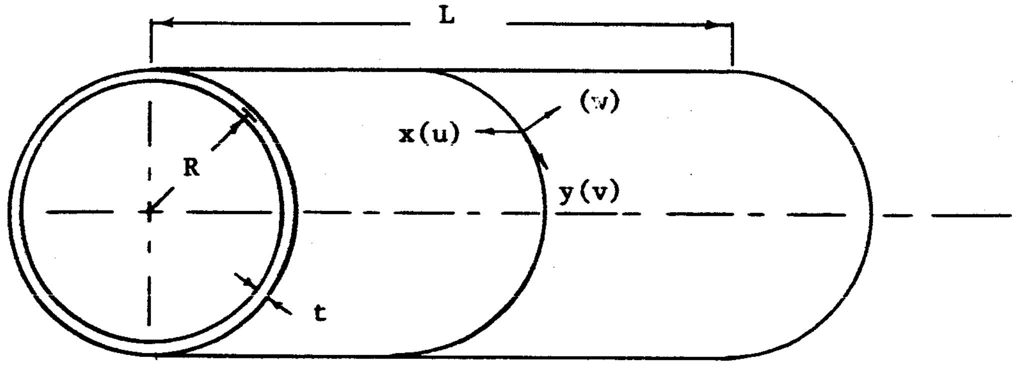

Fig. 3a. Coordinates x, y, z and Displacements u, v, w.

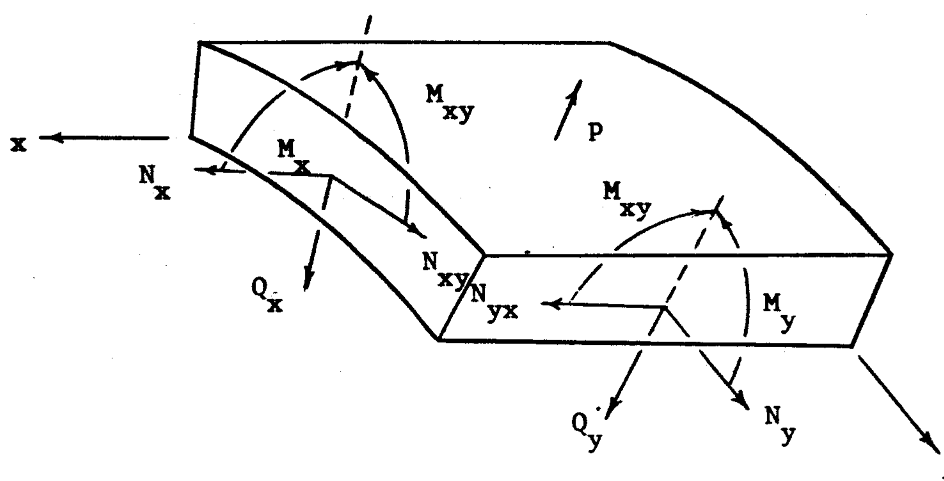

Fig. 3b. Forces and Moments on Element of Wall (p = Internal Pressure).

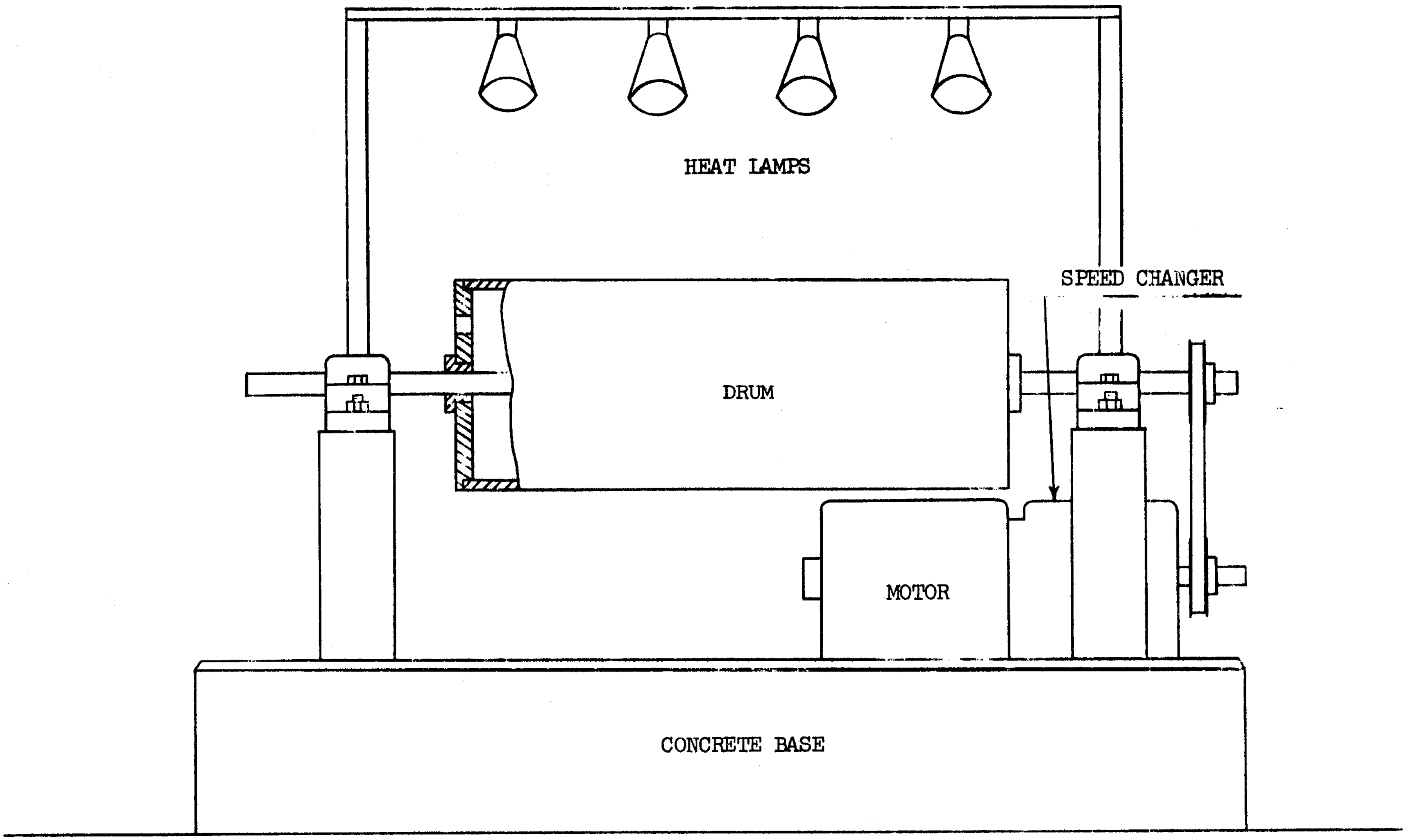

Fig. 4. SPINNING DRUM ASSEMBLY

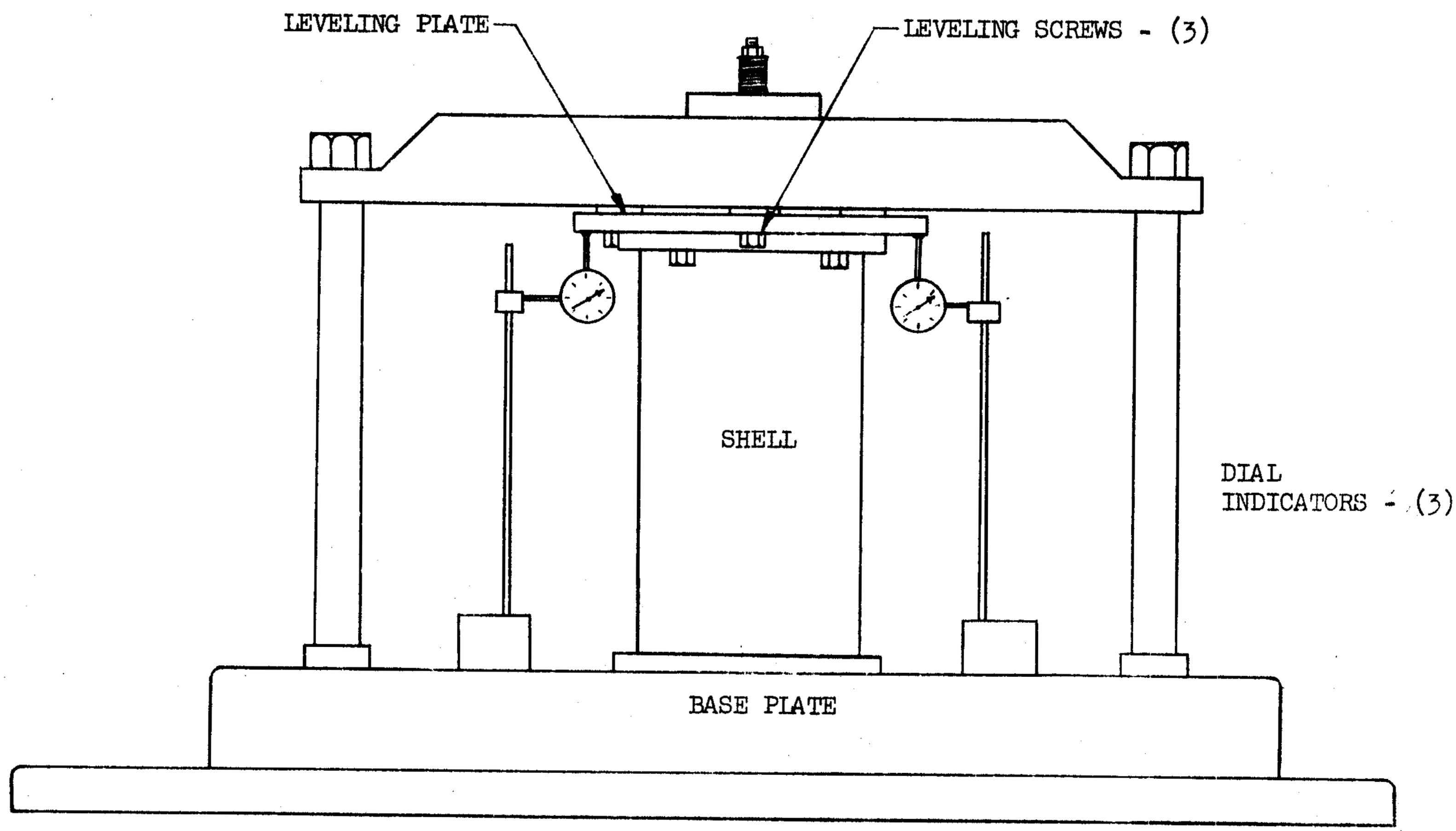

Fig. 5. Axial Testing Facility for Thin Walled Cylindrical Shells.

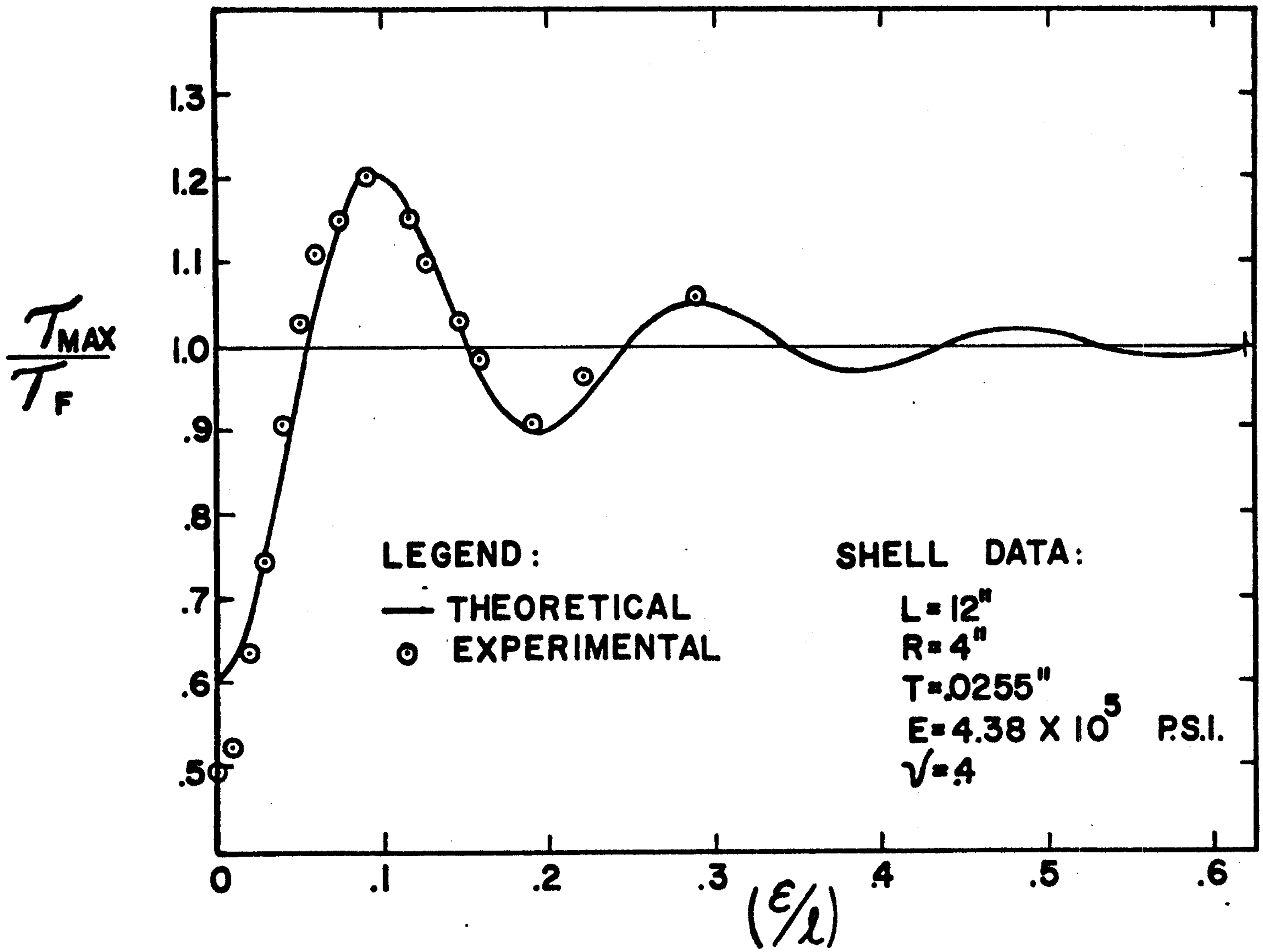

Fig. 6. Computed Ratio of Maximum Shear Stress Resultant to Maximum Shear Stress Resultant with Edge Effects Neglected, for Shell Loaded Axially to 90% of Classical Buckling Load.

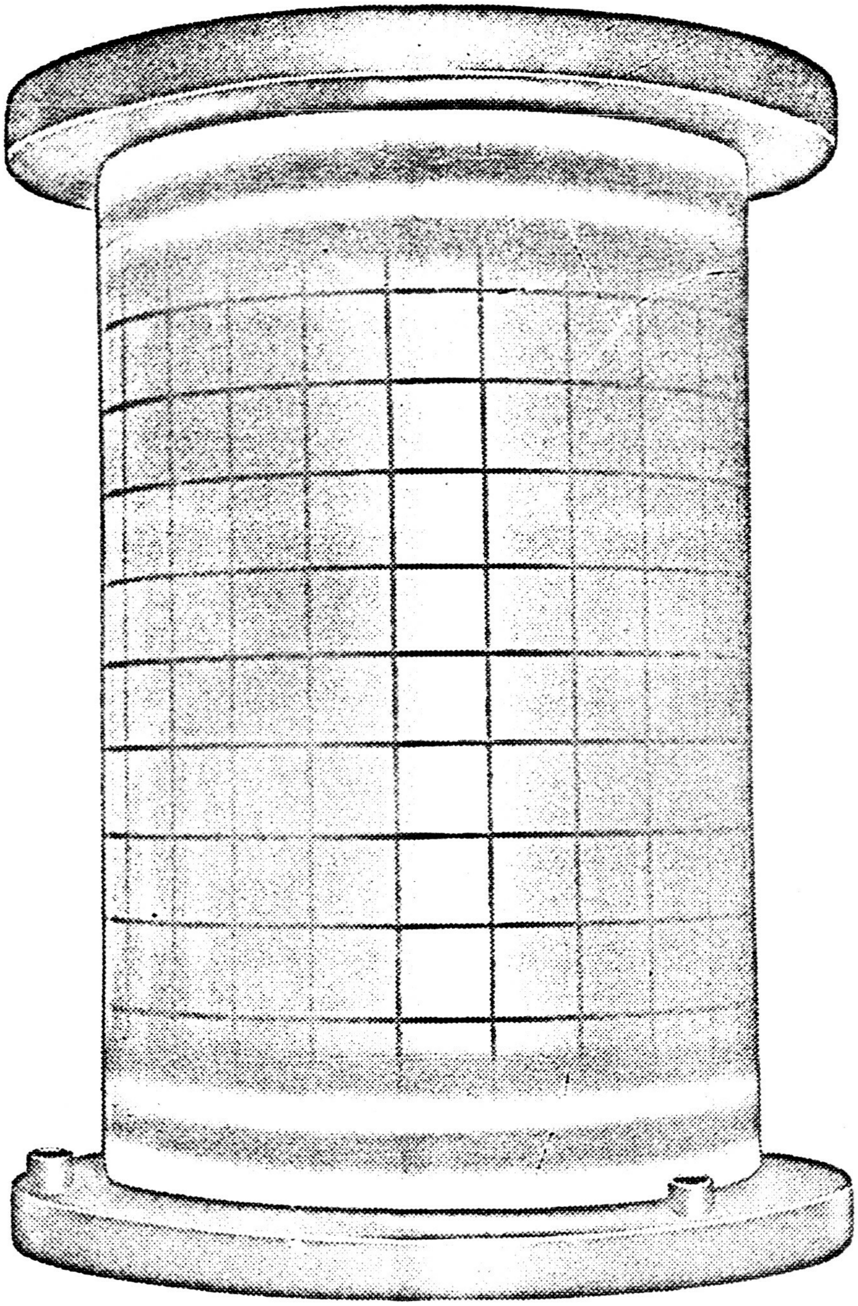

Fig. 7. View of Isochromatics of a Thin Cylindrical Shell Subjected to Axial Loading Equal to 90% of the Classical Buckling Load.

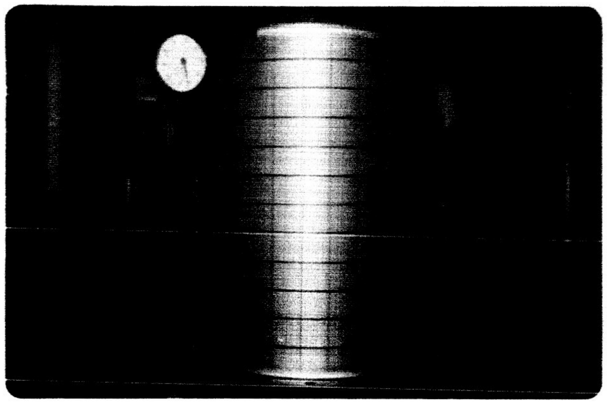

Fig. 8a. View of Prebuckled Cylindrical Shell Isochromatics.

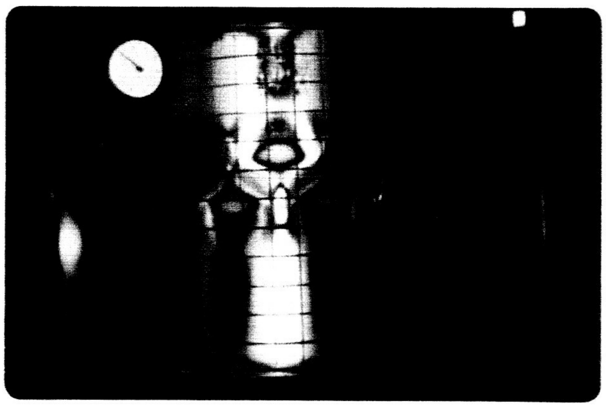

Fig. 8b. View of Post-buckled Cylindrical Shell Isochromatics.

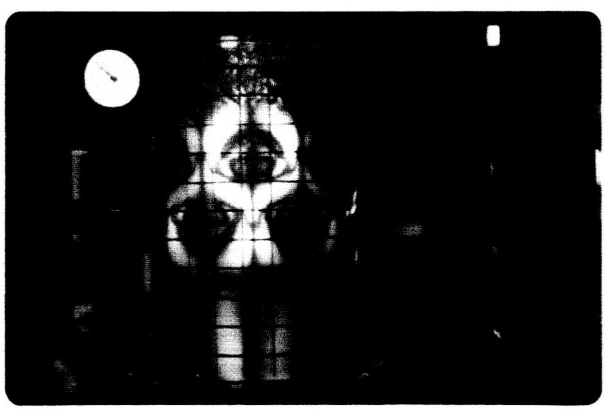

Fig. 8c. View of Post-buckled Cylindrical Shell 90° Isoclinics.

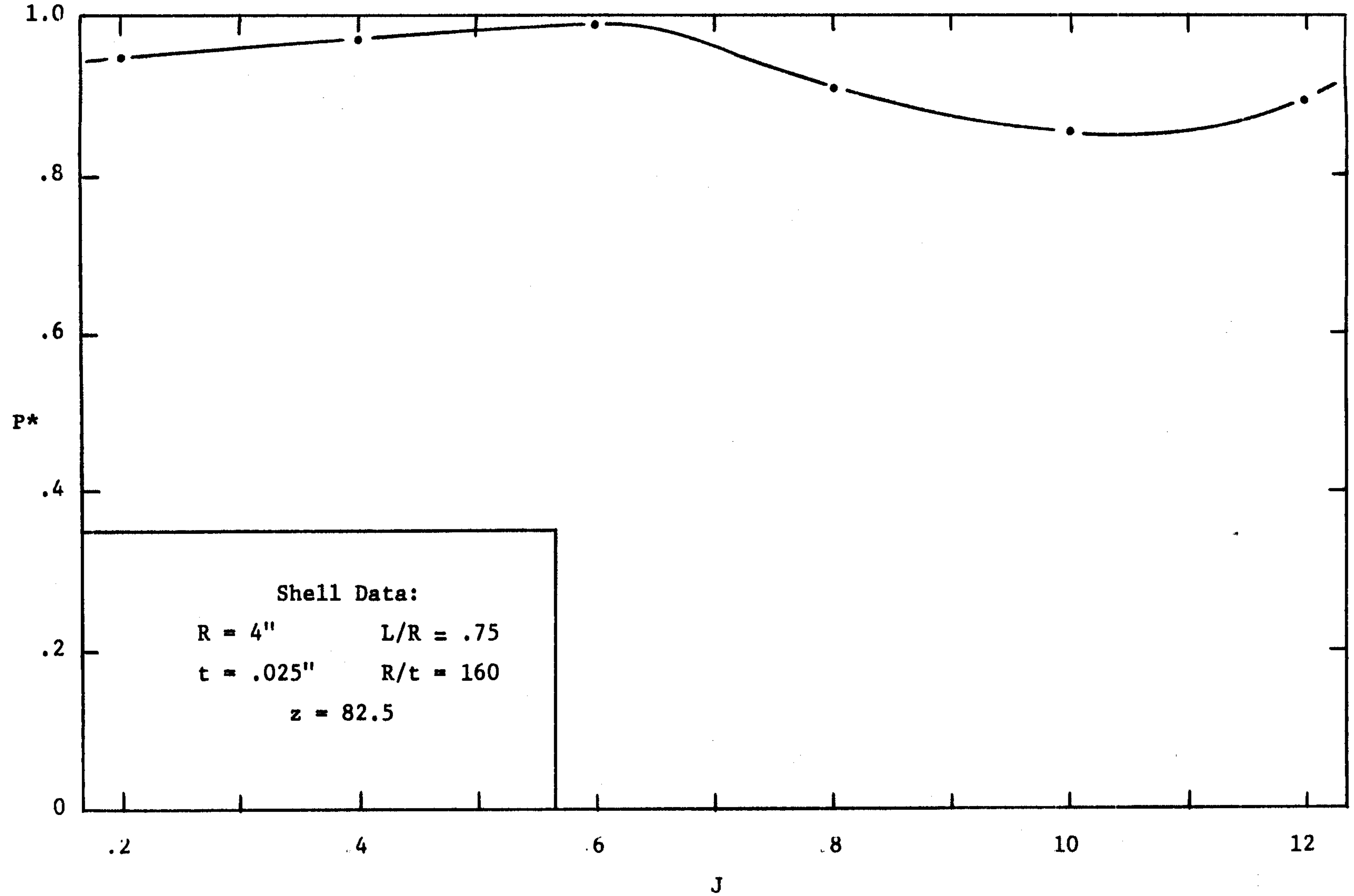

Fig. 9. Buckling of an Unpressurized Cylindrical Shell for Various Values of J. Analysis Based on 12 Term Expansion.

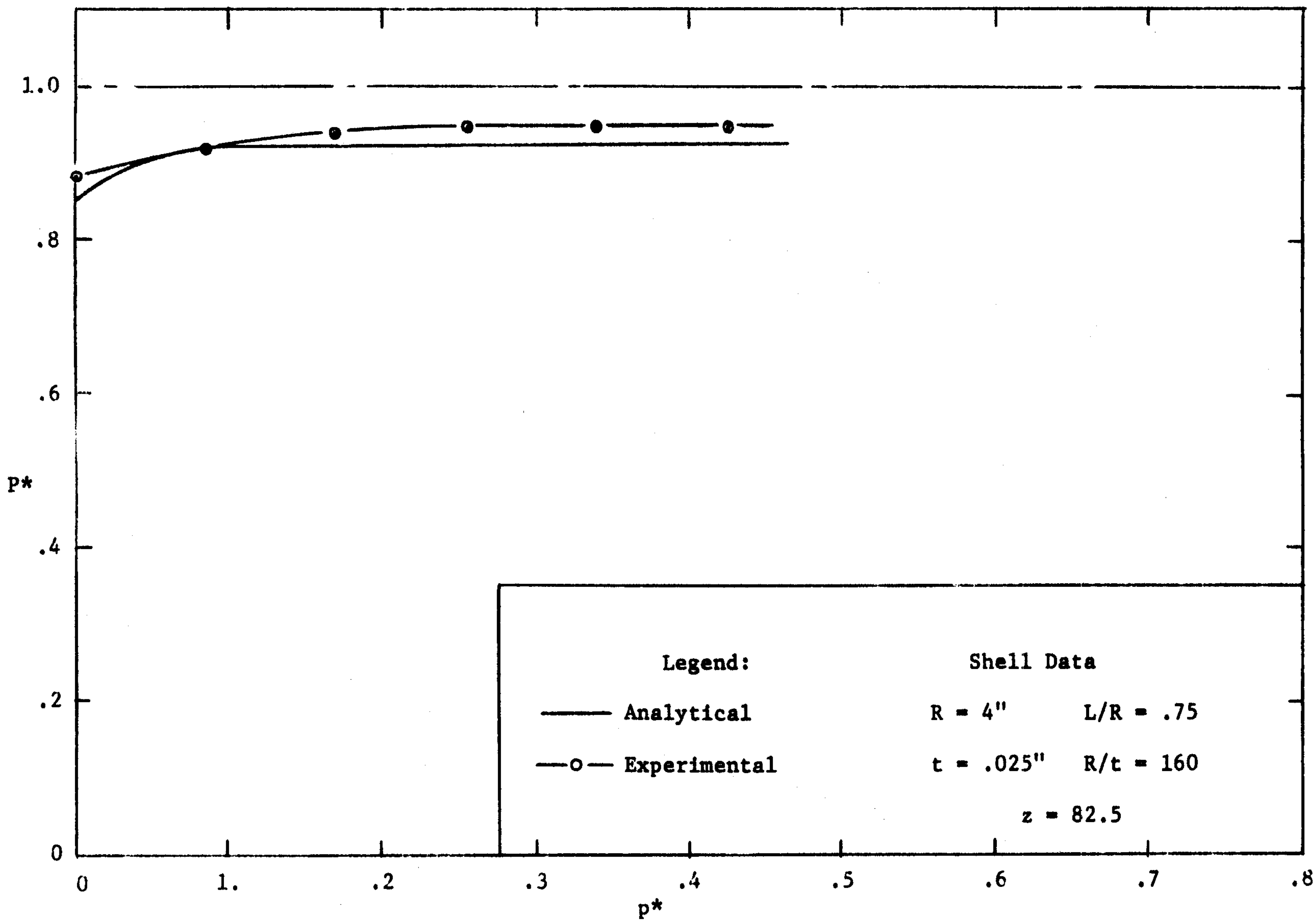

Fig. 10. Buckling of a Cylindrical Shell under Combinations of Axial Loading and Internal Pressure. J Varied to Minimize P* Throughout.

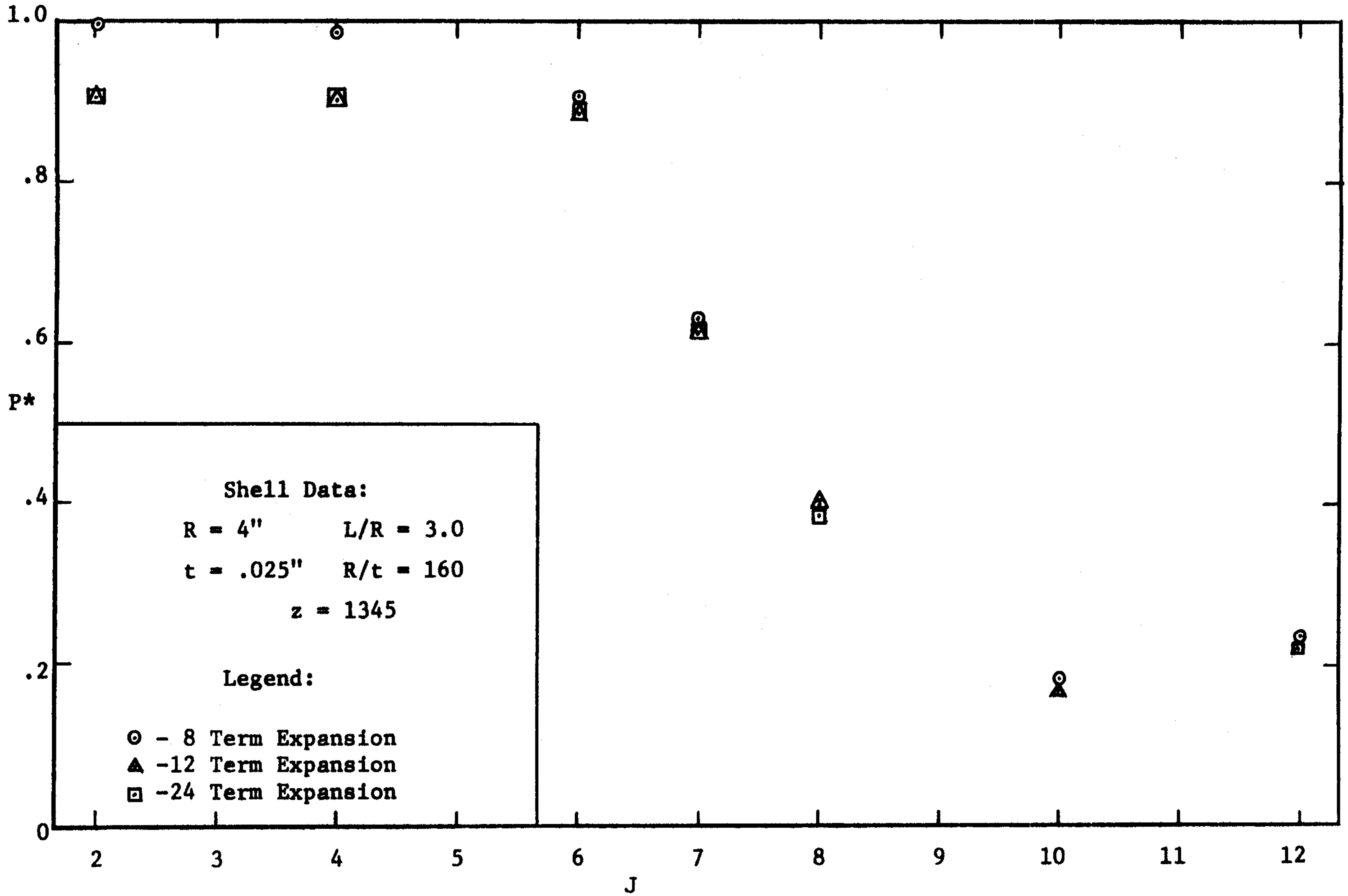

Fig. 11. Buckling of an Unpressurized Cylindrical Shell for Various Values of J.

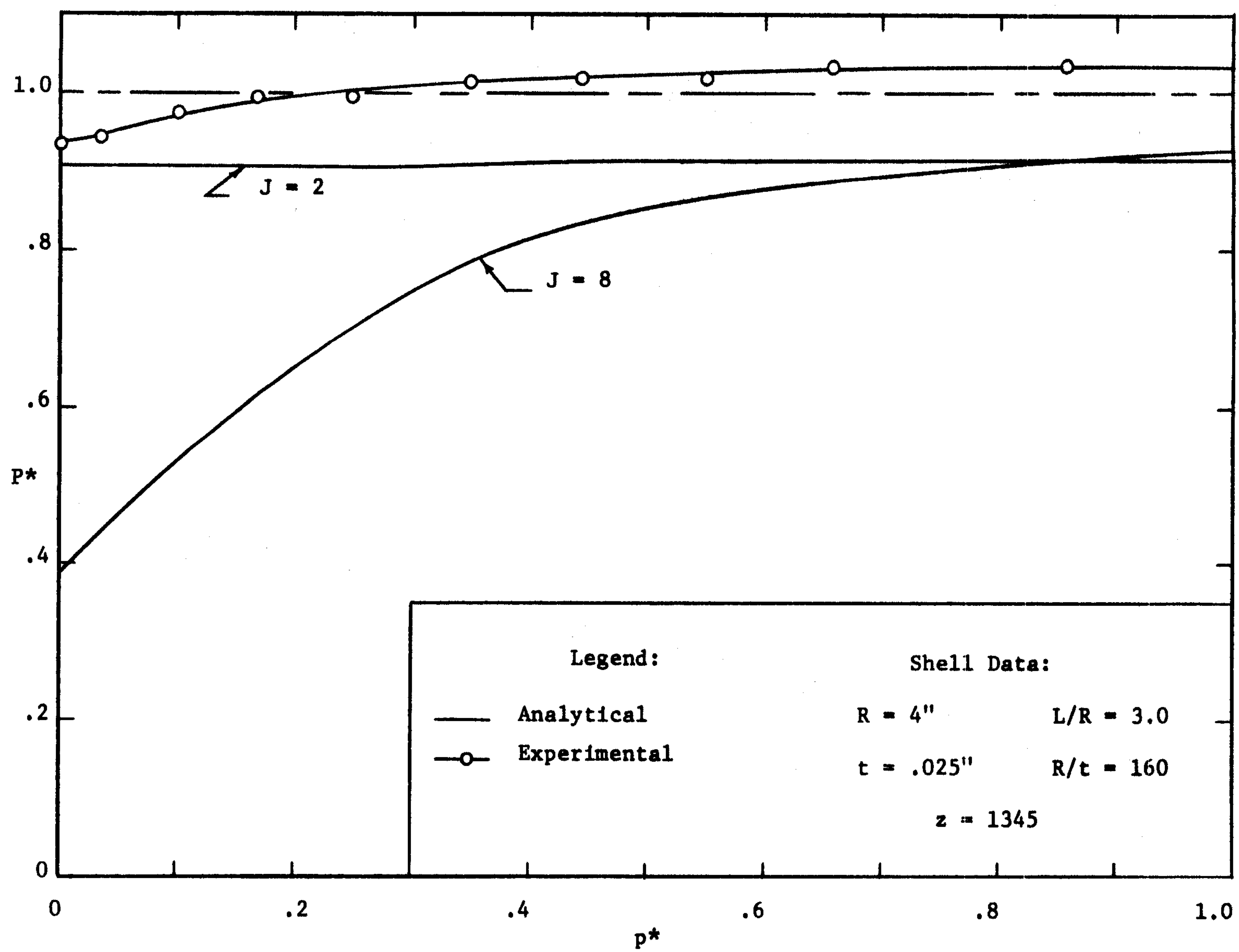

Fig. 12. Buckling of a Cylindrical Shell under Combinations of Axial Loading and Internal Pressure. Analysis Based on J = 2 and J = 8.

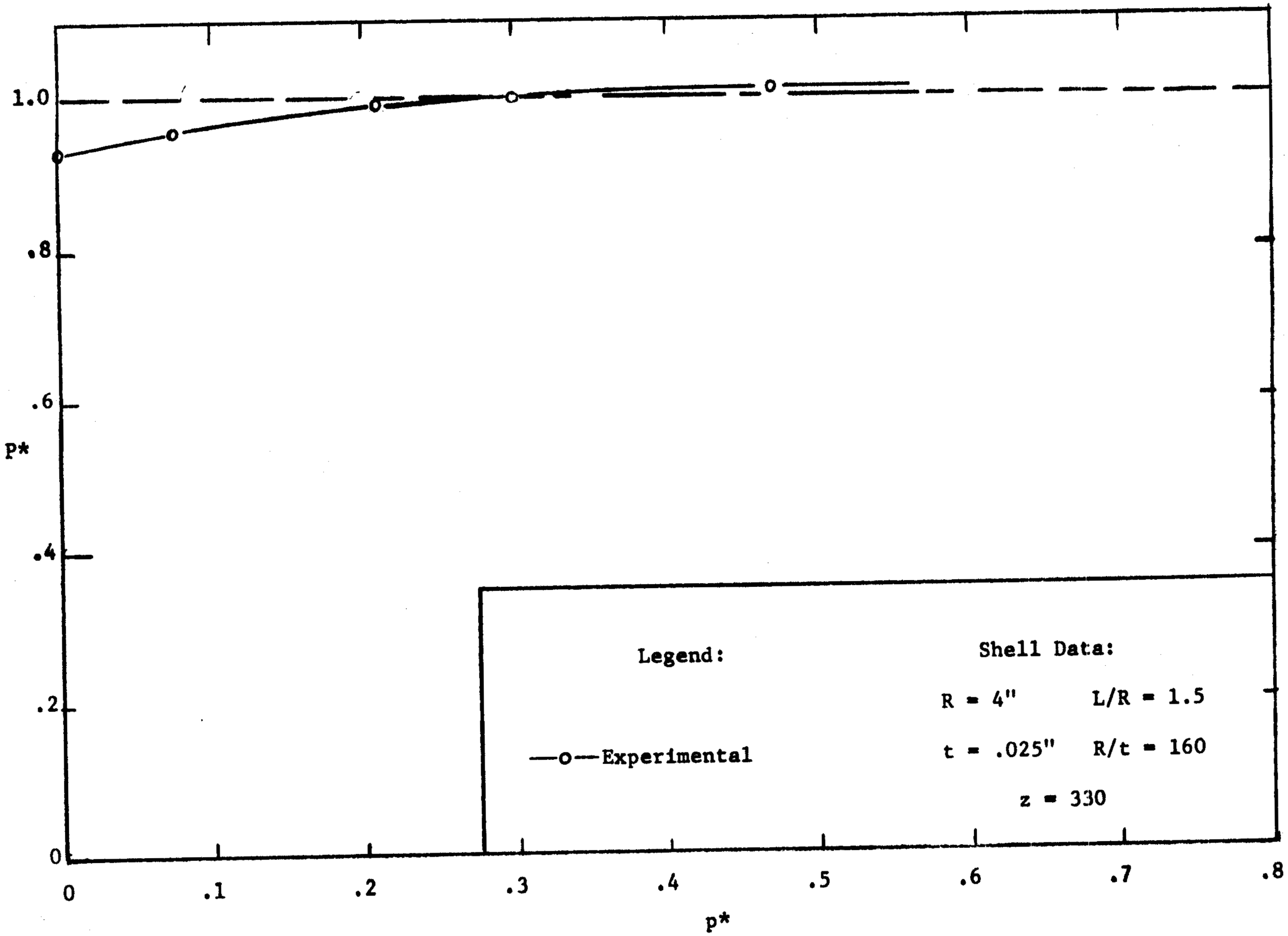

Fig. 13. Buckling of a Cylindrical Shell under Combinations of Axial Loading and Internal Pressure.

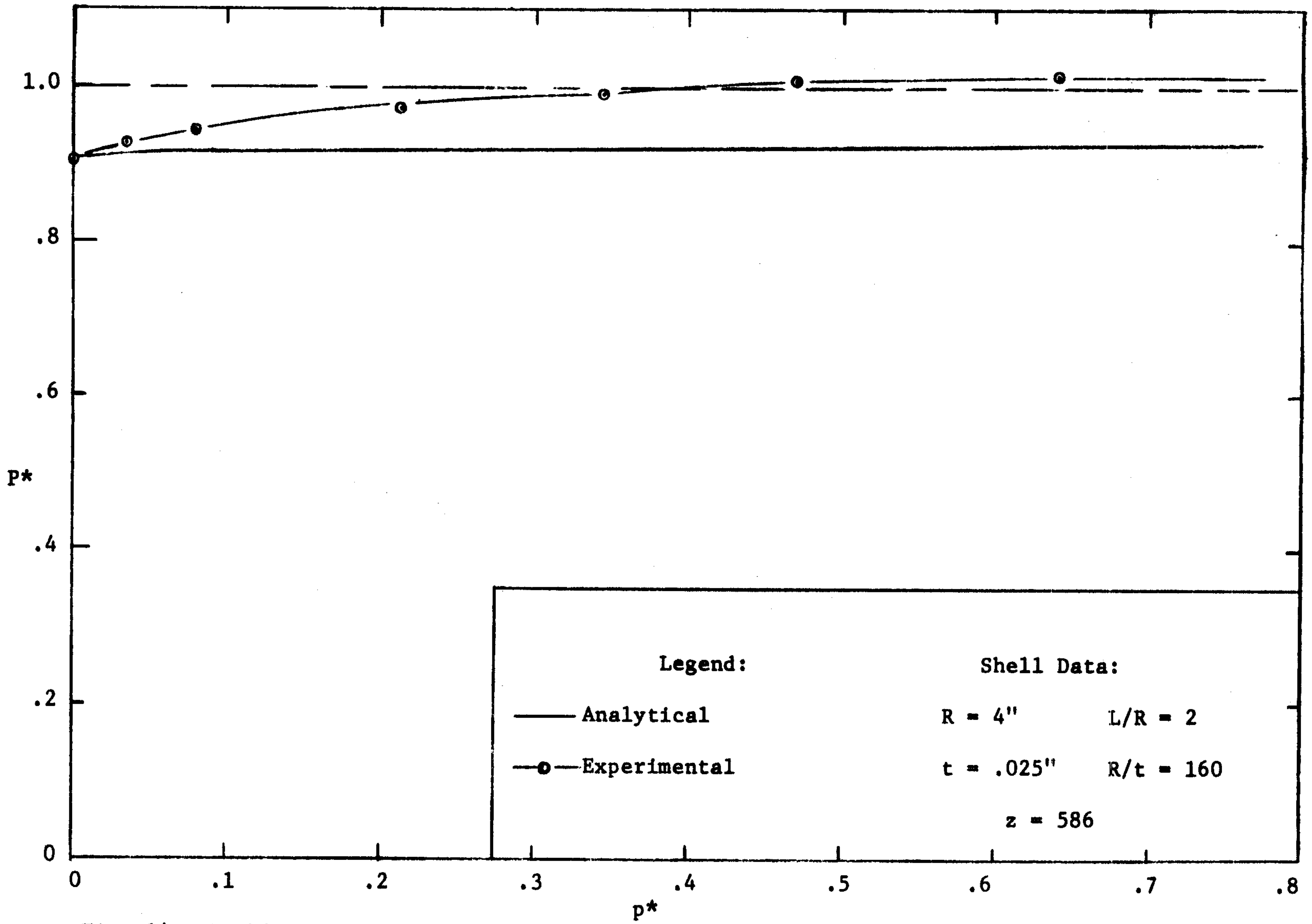

Fig. 14. Buckling of a Cylindrical Shell under Combinations of Axial Loading and Internal Pressure. Analysis Based on J = 2.

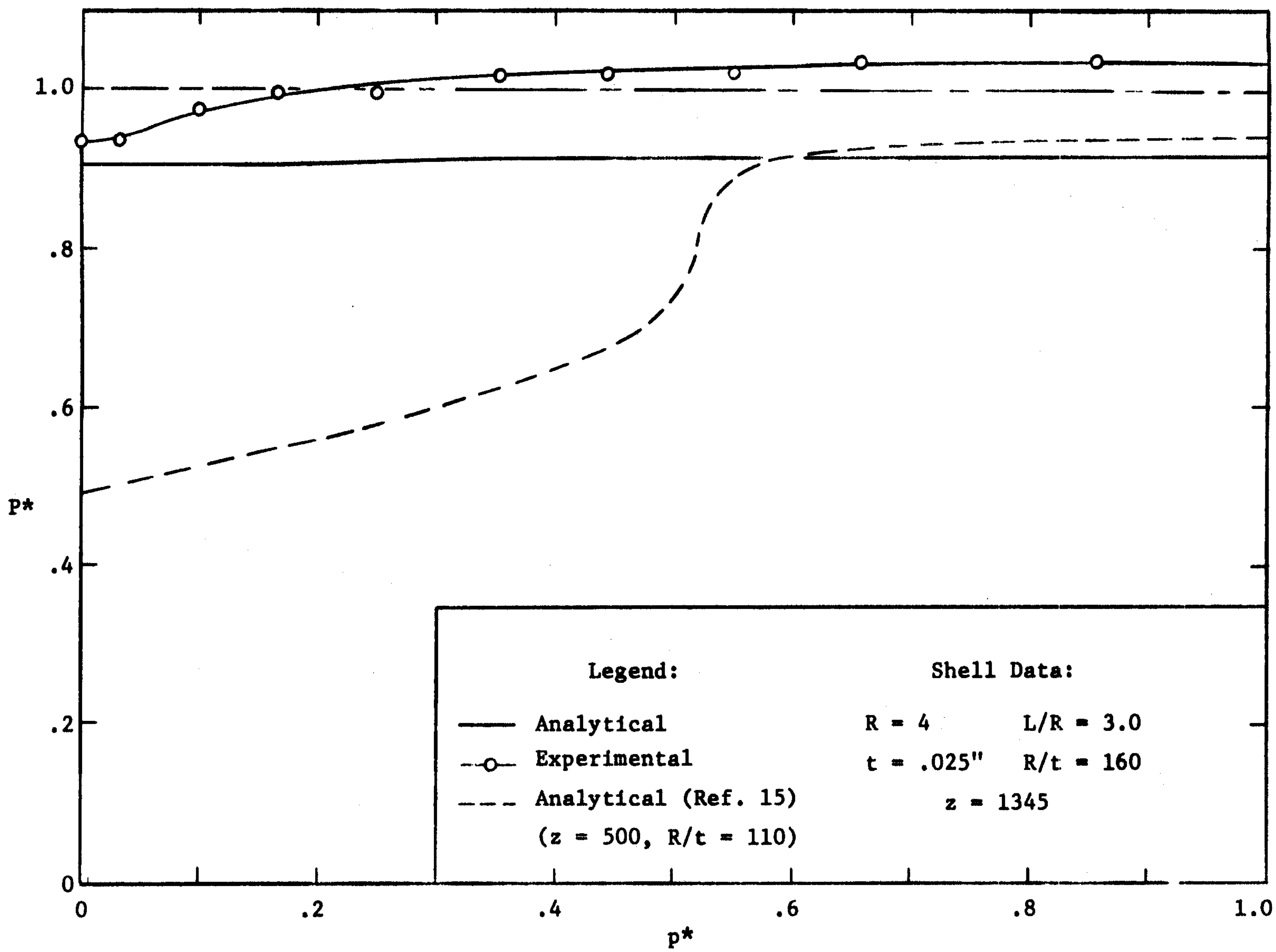

Fig. 15. Buckling of a Cylindrical Shell under Combinations of Axial Loading and Internal Pressure. Analysis Based on J = 2.

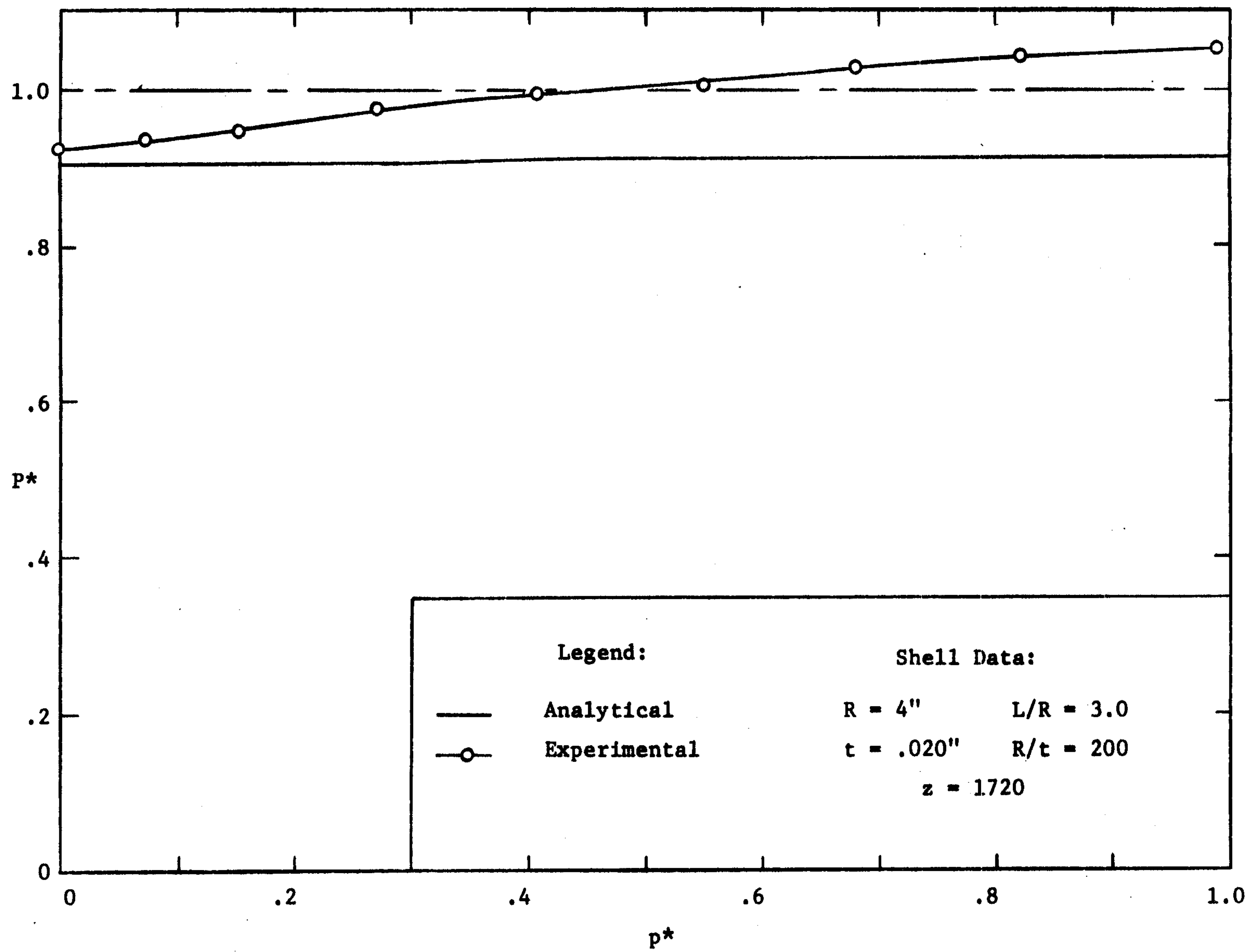

Fig. 16. Buckling of a Cylindrical Shell under Combinations of Axial Loading and Internal Pressure. Analysis Based on J = 2.

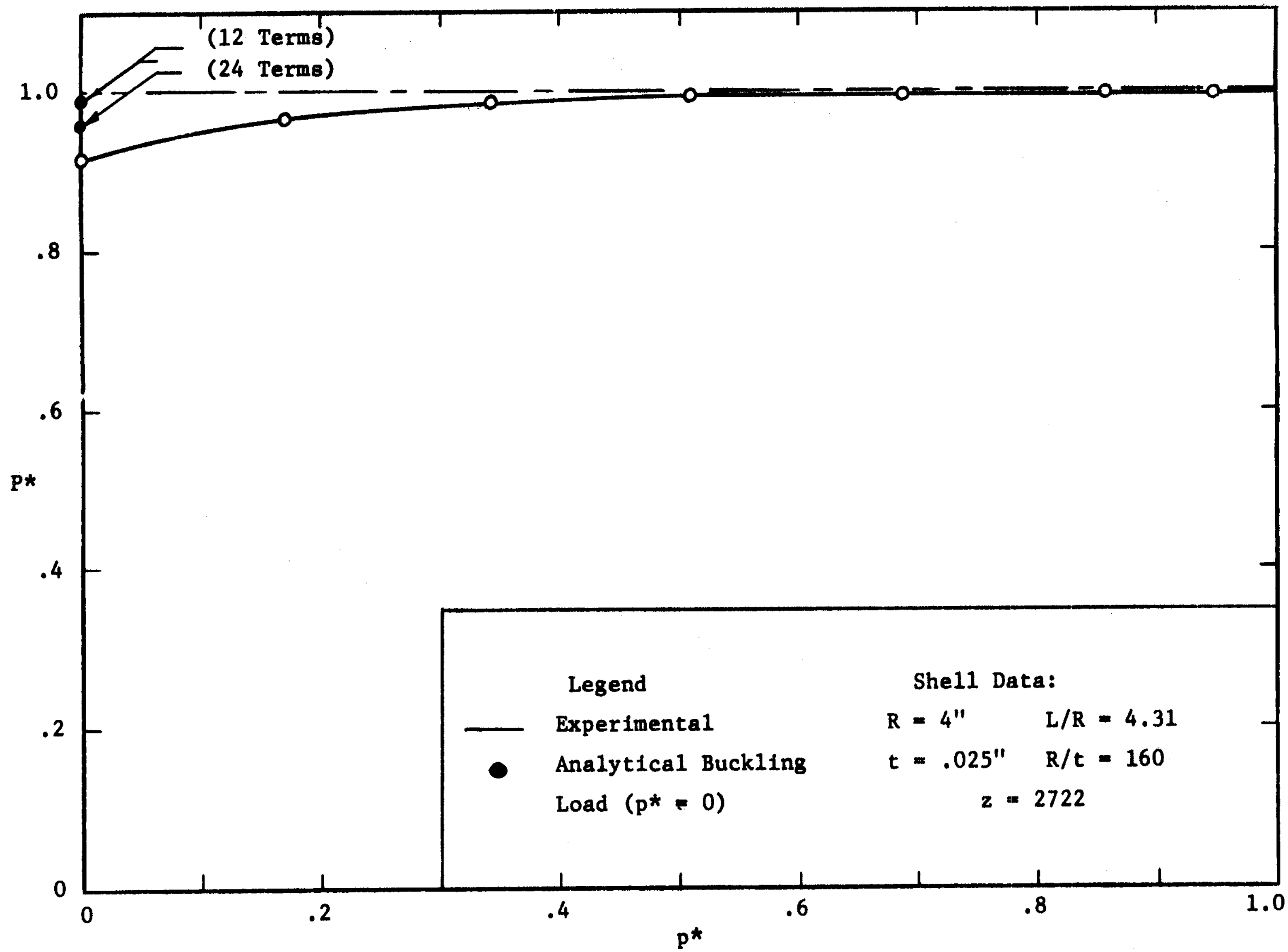

Fig. 17. Buckling of a Cylindrical Shell under Combinations of Axial Loading and Internal Pressure. Analysis Based on J = 2.

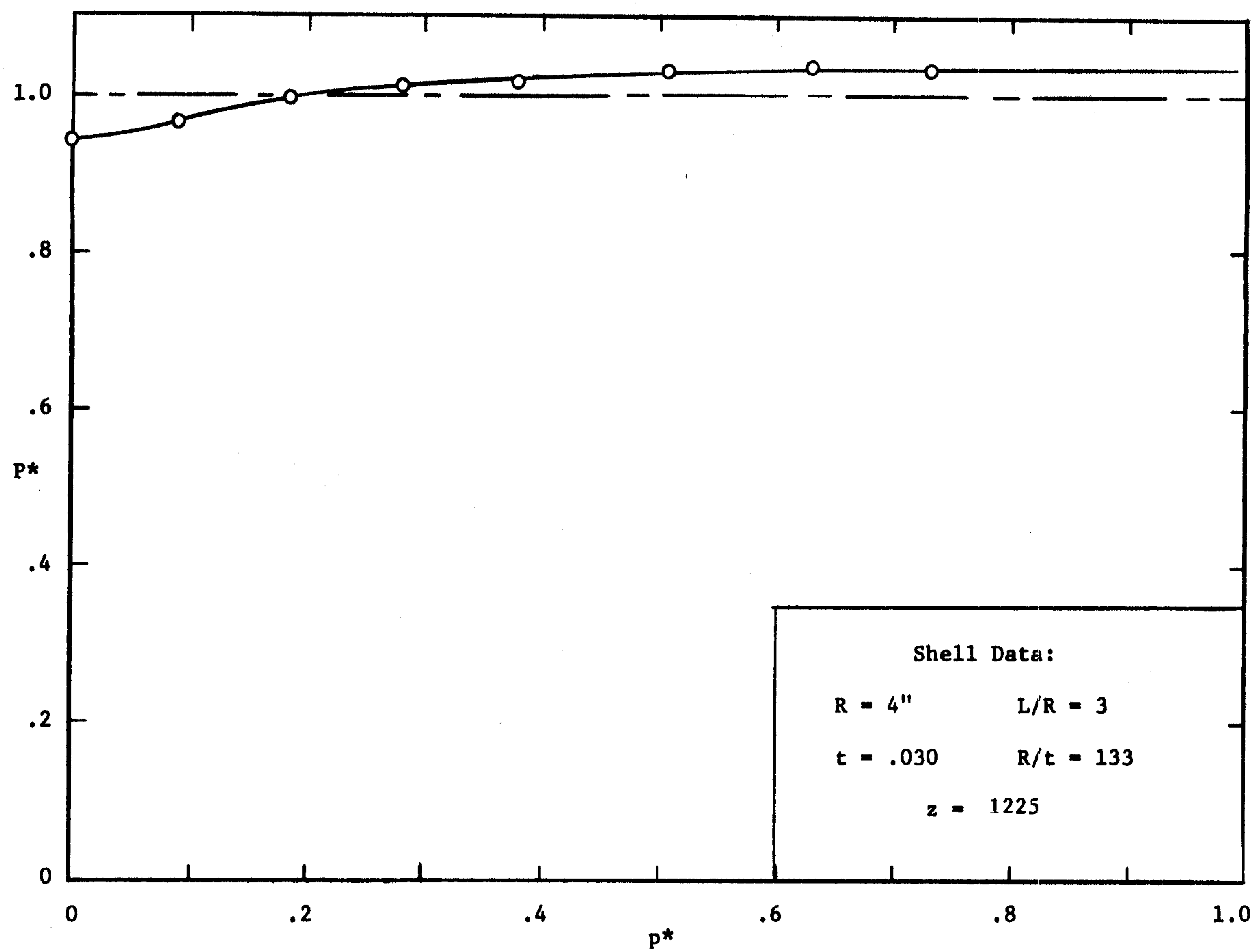

Fig. 18. **Buckling of a Cylindrical Shell under Combinations of Axial Loading and Internal Pressure. (Experimental)**

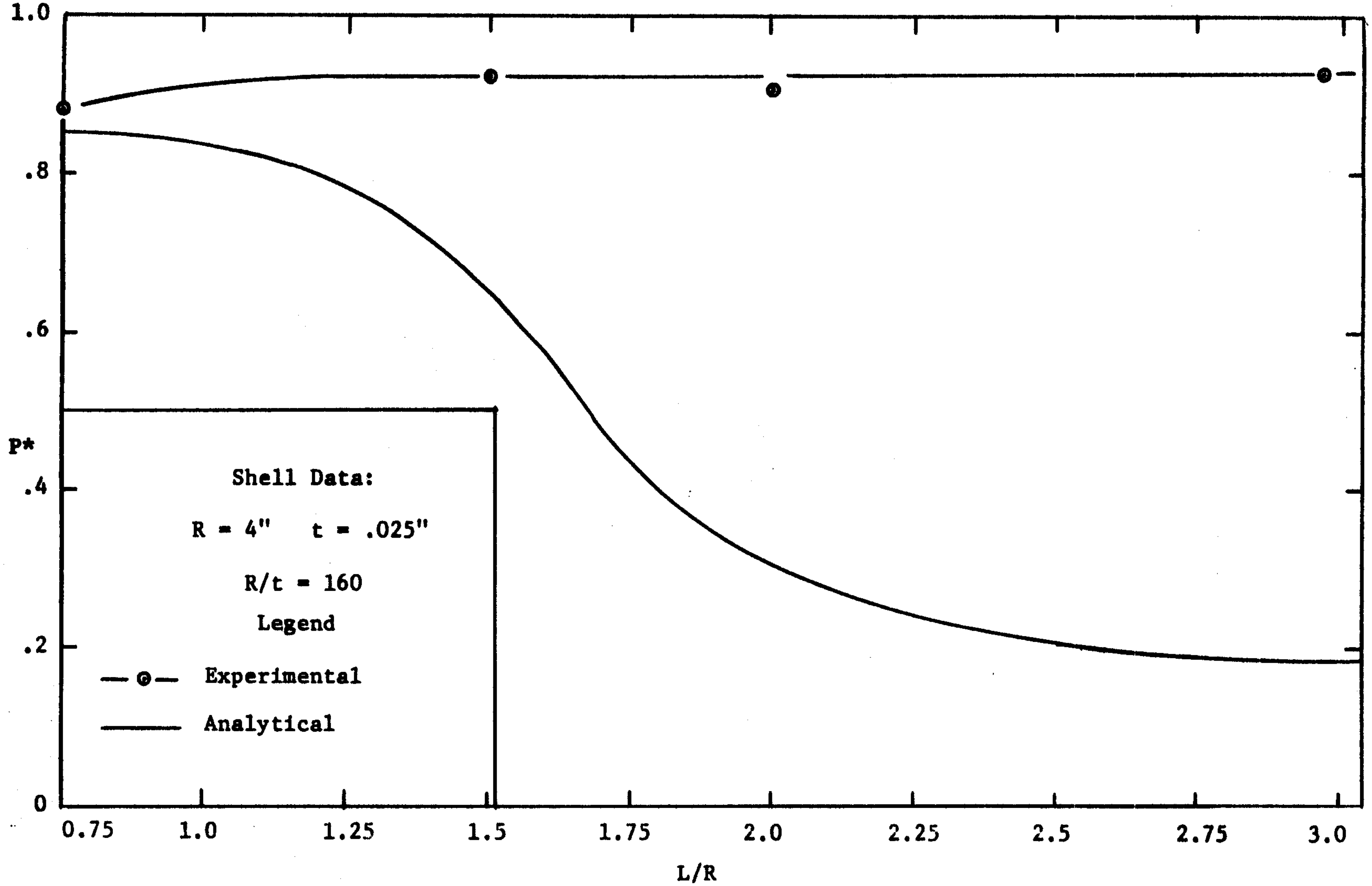

Fig. 19. Buckling of Unpressurized Cylindrical Shells. Analysis Carried out with J =10; 12 Terms in Expansions.

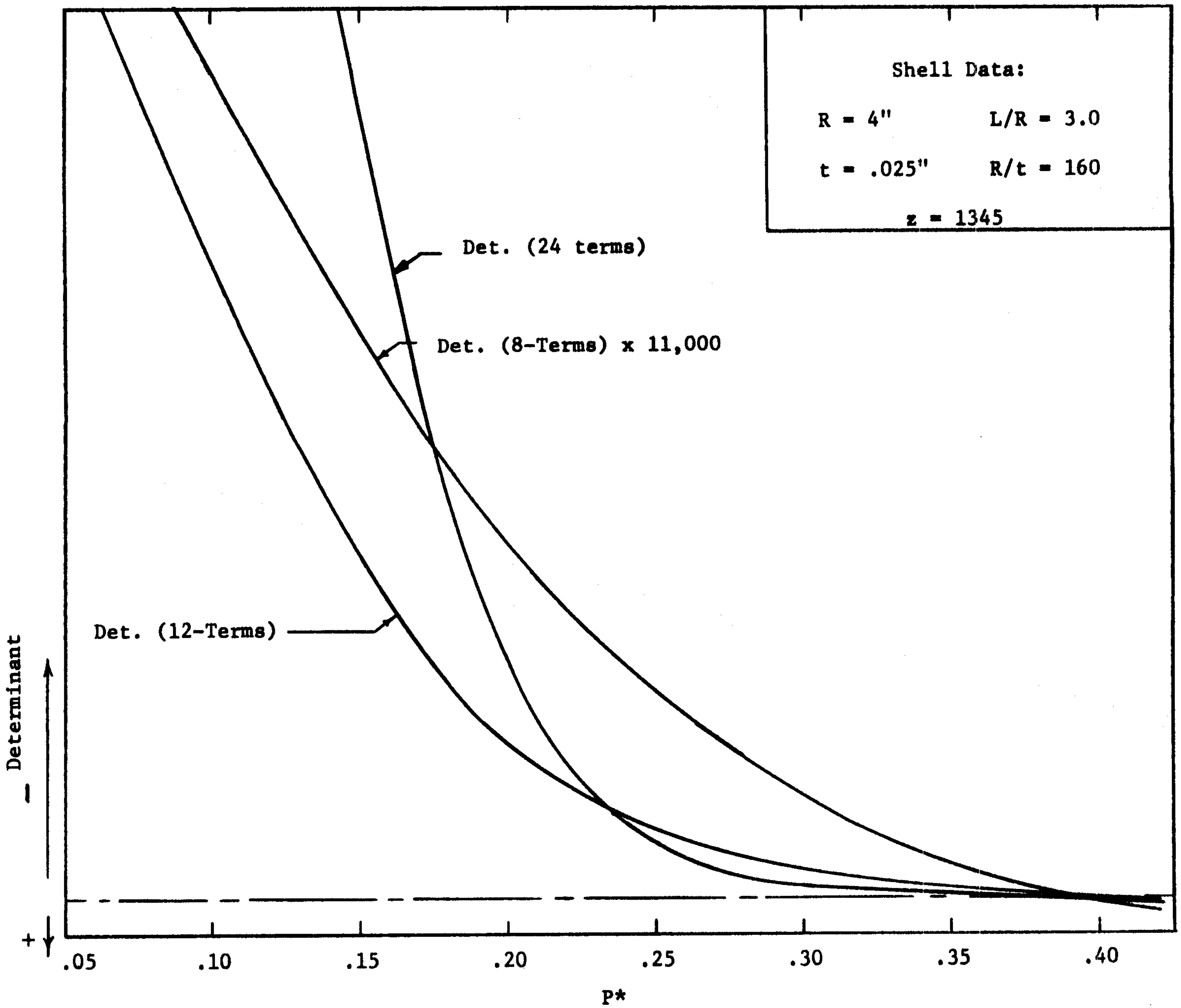

Fig. 20a. Determinant vs. P* for 8 and 12 Term Expansions with J = 8 and p = 0.

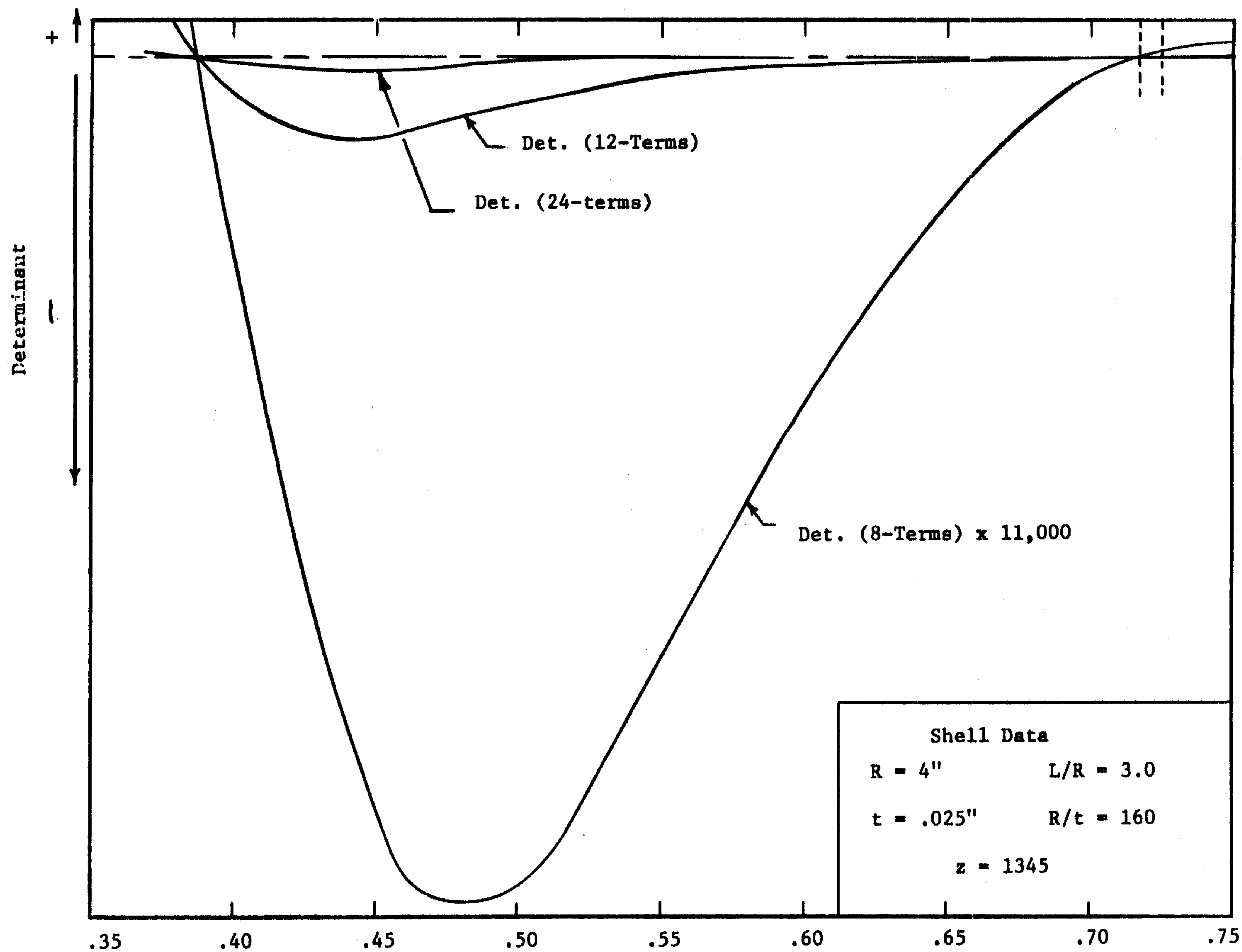

Fig. 20b. Determinant vs. P* for 8 and 12 Term Expansions with J = 8 and p = 0.

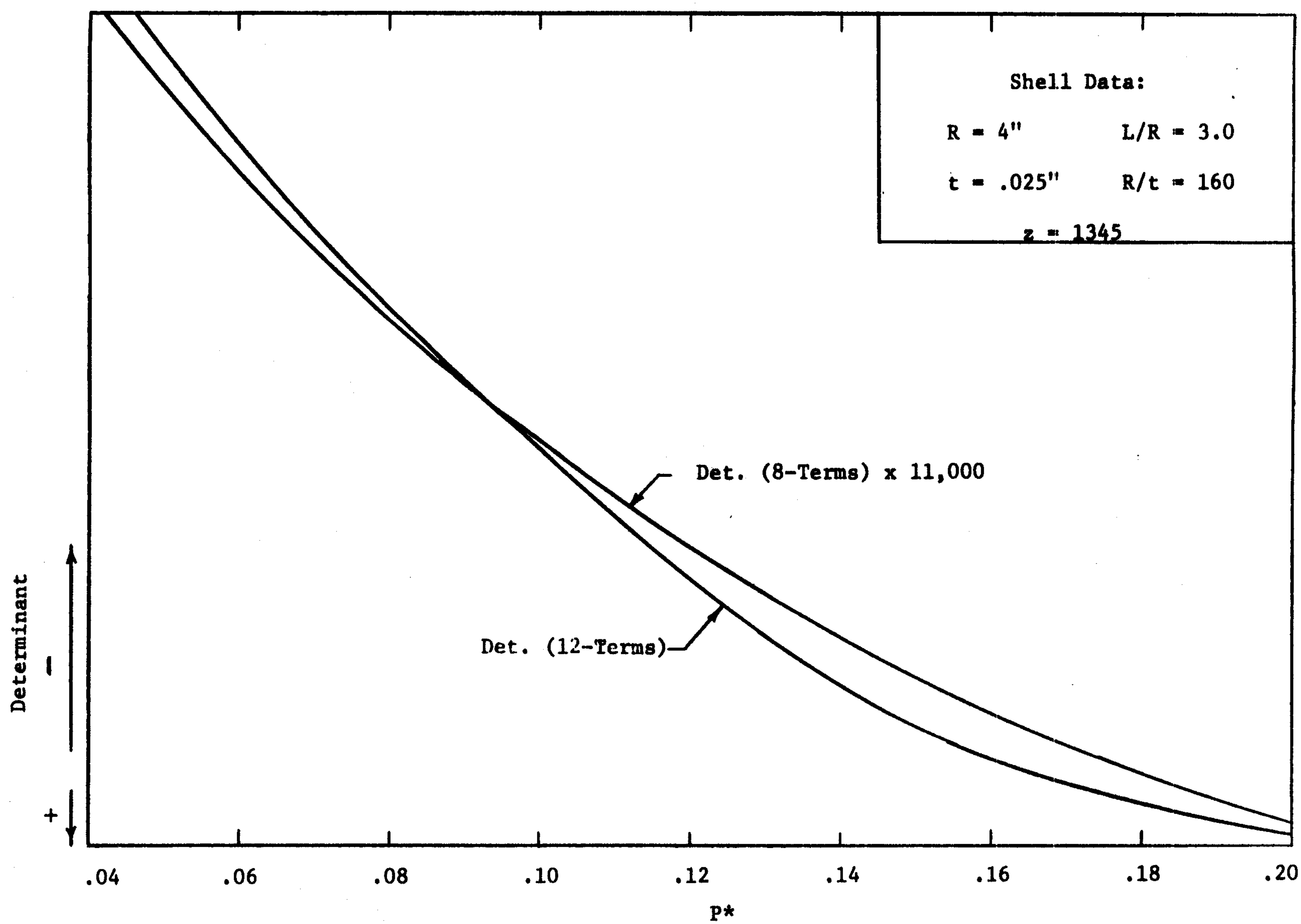

Fig. 21a. Determinant vs. P* for 8 and 12 Term Expansions with J = 10 and p = 0.

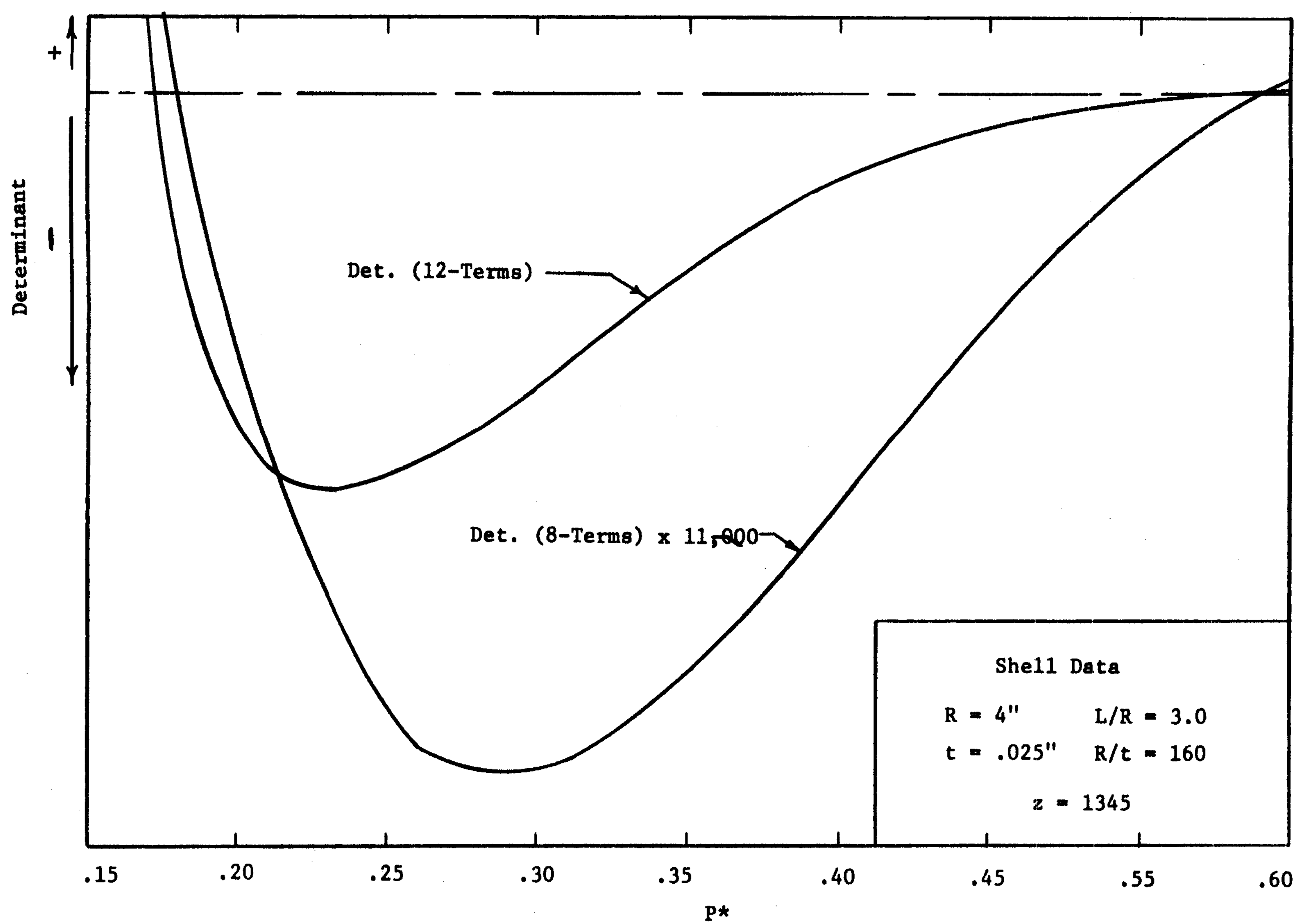

Fig. 21b. Determinant vs. P* for 8 and 12 Term Expansions with J = 10 and p = 0.

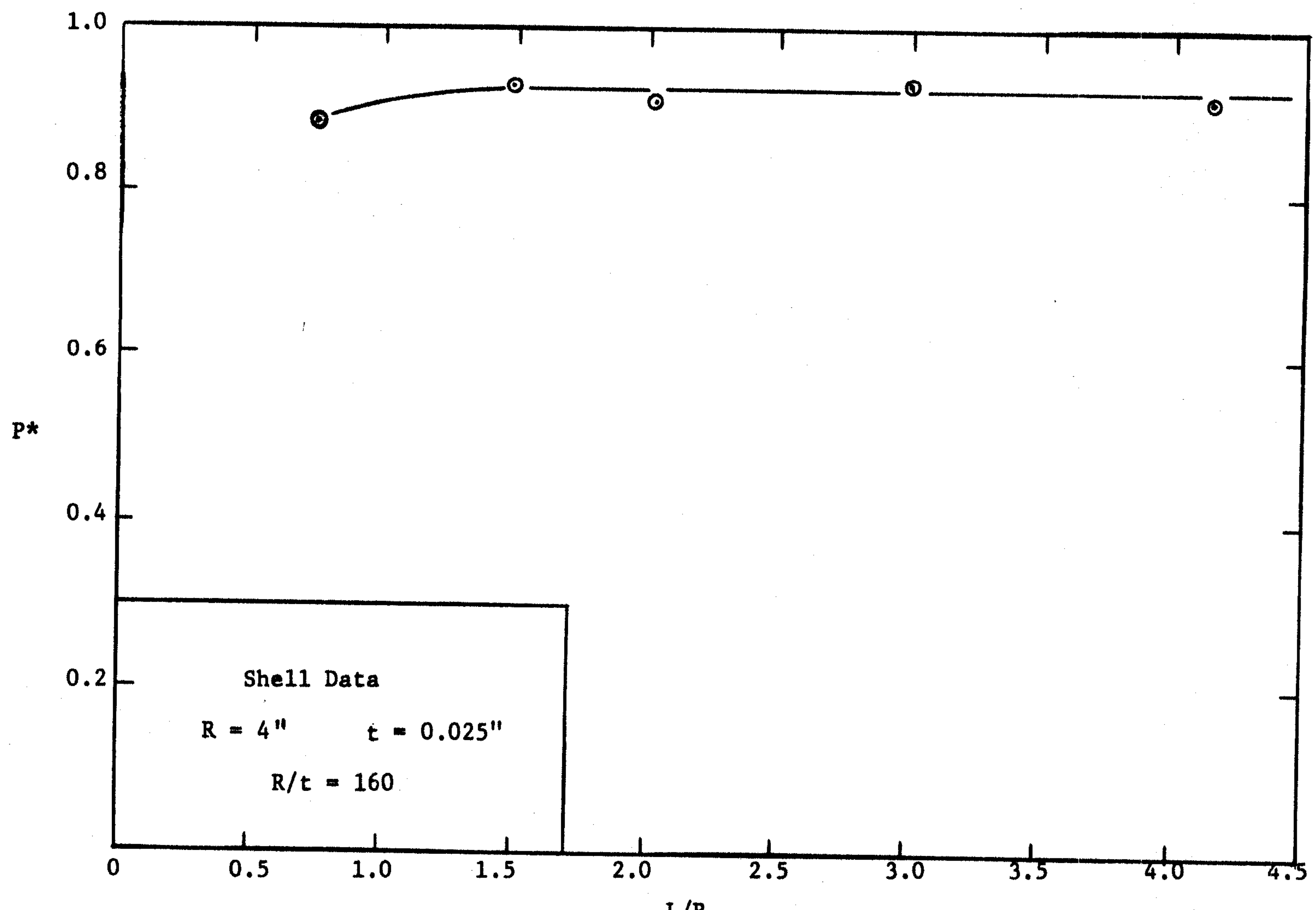

Fig. 22. Experimental Buckling Load vs. Ratio of Length to Radius for an Unpressurized Shell of Fixed Thickness ~~and Length~~.

APPENDIX A

Investigation of Number of Terms Required in Expansion

Results of the computations carried out in this paper indicate that, for longer shells subjected to no lateral loading, the analytic results deviate from experiment when the number of peripheral wave permitted is in the neighborhood of 10. Since the size of the matrices used herein was restricted to 72 x 72 one is led to investigate the possible effects of using larger matrices. In the finite difference methods used in Ref. [15] and [23] matrices of not less than 150 x 150 were employed when analysing the behavior of such shells.

As discussed earlier, since prebuckling deformation wavelengths are independent of shell length it is therefore to be expected that more terms in the buckling displacement expansions and hence larger matrices are to be required when analysing larger shells. In Fig. 19 the analytically predicted buckling load vs. ratio of shell length to radius, is plotted for a shell of fixed R/t, with J held constant at 10. We observed that the deviation from experiment is relatively small for L/R = 0.75 but increases rapidly as L/R increases. This observation is consistent with the contention that more terms in the expansions are required for larger shells, especially if a wide range of values of J are to be investigated.

The determinant vs. loading for J = 8 and J = 10, with different numbers of terms employed, has been plotted in Figs. 20a, 20b, 21a, and 21b, for a particular shell geometry with p = 0. In Figs. 20a, and 21a, the determinants have been scaled to give approximately the same magnitude and are plotted from

P* = 0.05 up to the first crossing of the axis. In Figs. 20b, and 21b, these determinants are plotted with their magnitudes in the same ratio as in the corresponding previous figures. The scale has been enlarged for clarity and the value of P* varies between the values associated with the first and second crossing of the axis.

We note in these figures that for the 12 term expansion the "dip" below the axis is much less than for the expansion of 8 terms. This would appear to indicate that with sufficient terms taken the "dip" would pull completely above the axis and hence remove the two lowest zeros from the results. The analysis would then give fair agreement with experiment.

APPENDIX B

Fortran-Pitt Computer Program (Print-out)

```
** H MOUNT SCRATCH   ON DRIVE 24 WITH RING ON
** T THIS PROGRAM LOADS SCRATCH TAPE  ON DR 24 FOR NEXT PROG,M         66
*    COMPILE FORTRAN,EXECUTE FORTRAN,DUMP IF ERROR
SUBROUTINECADD(AR,AI,BR,BI,CR,CI)
   CR DEFINED BUT NOT USED IN AN ARITH STMNT.
   CI DEFINED BUT NOT USED IN AN ARITH STMNT.
SUBROUTINECSUBT(AR,AI,BR,BI,CR,CI)
   CR DEFINED BUT NOT USED IN AN ARITH STMNT.
   CI DEFINED BUT NOT USED IN AN ARITH STMNT.
SUBROUTINECMULT(AR,AI,BR,BI,CR,CI)
   CR DEFINED BUT NOT USED IN AN ARITH STMNT.
   CI DEFINED BUT NOT USED IN AN ARITH STMNT.
SUBROUTINECDIV(AR,AI,BR,BI,CR,CI)
   CR DEFINED BUT NOT USED IN AN ARITH STMNT.
   CI DEFINED BUT NOT USED IN AN ARITH STMNT.
SUBROUTINESINH(AR,AI,BR,BI)
SUBROUTINECOSH(AR,AI,BR,BI)
SUBROUTINEEZ(AR,AI,BR,BI)
   BR DEFINED BUT NOT USED IN AN ARITH STMNT.
   BI DEFINED BUT NOT USED IN AN ARITH STMNT.
SUBROUTINECSCS(A1,A2,A3,A4,EL,C1,S1,VAL)
  VAL DEFINED BUT NOT USED IN AN ARITH STMNT.
SUBROUTINESSCS(A1,A2,A3,A4,EL,C1,S1,VAL)
  VAL DEFINED BUT NOT USED IN AN ARITH STMNT.
SUBROUTINESSCC(A1,A2,A3,A4,EL,C1,S1,VAL)
  VAL DEFINED BUT NOT USED IN AN ARITH STMNT.
SUBROUTINECSCC(A1,A2,A3,A4,EL,C1,S1,VAL)
  VAL DEFINED BUT NOT USED IN AN ARITH STMNT.
SUBROUTINECCCC(A1,A2,A3,A4,EL,C1,S1,VAL)
  VAL DEFINED BUT NOT USED IN AN ARITH STMNT.
SUBROUTINESSSS(A1,A2,A3,A4,EL,C1,S1,VAL)
  VAL DEFINED BUT NOT USED IN AN ARITH STMNT.
*** MAIN PROGRAM ***
    K DEFINED BUT NOT USED IN AN ARITH STMNT.
2000       SUBROUTINE CADD(AR,AI,BR,BI,CR,CI)
2006       CR=AR+BR
2009       CI=AI+BI
2012       RETURN
     0005865028
           END
2033       SUBROUTINE CSUBT(AR,AI,BR,BI,CR,CI)
2039       CR=AR-BR
2042       CI=AI-BI
2045       RETURN
           END
2066       SUBROUTINE CMULT(AR,AI,BR,BI,CR,CI)
2072       A1=AR
2074       A2=AI
2076       B1=BR
2078       B2=BI
2080       CR=A1*B1-A2*B2
2087       CI=A1*B2+A2*B1
2094       RETURN
           END
2120       SUBROUTINE CDIV (AR,AI,BR,BI,CR,CI)
2126       A1=AR
2128       A2=AI
2130       B1=BR
```

```
      B2=BI
       D=BR*BR+BI*BI
      IF (D) 1,2,1
    2 PRINT 3
    3 FORMAT (12HCDIV BY ZERO)
    1 CR=(A1*B1+A2*B2)/D
       CI=(A2*B1-A1*B2)/D
      END
      SUBROUTINE SINH (AR,AI,BR,BI)
      CALL EZ(AR,AI,CR,CI)
      CALL EZ(-AR,-AI,DR,DI)
      CALL CSUBT(CR,CI,DR,DI,BR,BI)
      BR=BR/2.
      BI=BI/2.
      RETURN
      END
      SUBROUTINE COSH(AR,AI,BR,BI)
      CALL EZ(AR,AI,CR,CI)
      DR=-AR
      DI=-AI
      CALL EZ(DR,DI,BR,BI)
      CALL CADD(CR,CI,BR,BI,BR,BI)
      BR=BR/2.
      BI=BI/2.
      RETURN
      END
      SUBROUTINE  EZ(AR,AI,BR,BI)
      EAR=EXPEF(AR)
      BR=EAR*COSF(AI)
      BI=EAR*SINF(AI)
      RETURN
      END
      SUBROUTINE CSCS(A1,A2,A3,A4,EL,C1,S1,VAL)
       X=A2+A3-A4
      W1=(C1*X*SINF(X*EL))/((A1*A1)+(X*X))
      W2=(S1*A1*COSF(X*EL))/((A1*A1)+(X*X))
       X=A2+A3+A4
      W3=((C1*X*SINF(X*EL))+(S1*A1*COSF(X*EL)))/((A1*A1)+(X*X))
       X=A2-A3-A4
      W4=((C1*X*SINF(X*EL))+(S1*A1*COSF(X*EL)))/((A1*A1)+(X*X))
      X=A2-A3+A4
      W5=((C1*X*SINF(X*EL))+(S1*A1*COSF(X*EL)))/((A1*A1)+(X*X))
      VAL=(W1+W2-W3+W4-W5)/4.0
      RETURN
      END
      SUBROUTINE SSCS(A1,A2,A3,A4,EL,C1,S1,VAL)
      X=A2+A3-A4
      W1=(((S1*X *SINF(X*EL))+(C1*A1*COSF(X*EL)))-(    A1))/((A1*A1)+(X*X
     1))
      X=A2+A3+A4
      W2=(((S1*X*SINF(X*EL))+(C1*A1*COSF(X*EL)))-(    A1))/((A1*A1)+(X*X)
     1)
       X=A2-A3-A4
      W3=(((S1*X*SINF(X*EL))+(C1*A1*COSF(X*EL)))-(    A1))/((A1*A1)+(X*X)
     1)
       X=A2-A3+A4
      W4=((S1*X*SINF(X*EL))+(C1*A1*COSF(X*EL))-(    A1))/((A1*A1)+(X*X))
```

```
2638         VAL=(W1-W2+W3-W4)/(4.)
2647         RETURN
             END
2678         SUBROUTINE SSCC(A1,A2,A3,A4,EL,C1,S1,VAL)
2684         X=A2+A3-A4
2688         W1=((C1*A1*SINF(X*EL))-(S1*X*COSF(X*EL)))/((A1*A1)+(X*X))
2712         X=A2+A3+A4
2716         W2=((C1*A1*SINF(X*EL))-(S1*X*COSF(X*EL)))/((A1*A1)+(X*X))
2740         X=A2-A3-A4
2744         W3=((C1*A1*SINF(X*EL))-(S1*X*COSF(X*EL)))/((A1*A1)+(X*X))
2768         X=A2-A3+A4
2772         W4=((C1*A1*SINF(X*EL))-(S1*X*COSF(X*EL)))/((A1*A1)+(X*X))
2796         VAL=(W1+W2+W3+W4)/(4.)
2805         RETURN
             END
2835         SUBROUTINE CSCC(A1,A2,A3,A4,EL,C1,S1,VAL)
2841         X=A2-A3-A4
2845         W1=((S1*A1*SINF(X*EL))-(C1*X*COSF(X*EL))+(    X))/((A1*A1)+(X*X))
2870         X=A2-A3+A4
2874         W2=((S1*A1*SINF(X*EL))-(C1*X*COSF(X*EL))+(    X))/((A1*A1)+(X*X))
2899         X=A2+A3-A4
2903         W3=((S1*A1*SINF(X*EL))-(C1*X*COSF(X*EL))+(    X))/((A1*A1)+(X*X))
2928         X=A2+A3+A4
2932         W4=((S1*A1*SINF(X*EL))-(C1*X*COSF(X*EL))+(    X))/((A1*A1)+(X*X))
2957         VAL=(W1+W2+W3+W4)/(4.)
2966         RETURN
             END
2996         SUBROUTINE CCCC(A1,A2,A3,A4,EL,C1,S1,VAL)
3002         X=A2-A3+A4
3006         W1=((C1*X*SINF(X*EL))+(S1*A1*COSF(X*EL)))/((A1*A1)+(X*X))
3028         X=A2+A3-A4
3032         W2=((C1*X*SINF(X*EL))+(S1*A1*COSF(X*EL)))/((A1*A1)+(X*X))
3054         X=A2-A3-A4
3058         W3=((C1*X*SINF(X*EL))+(S1*A1*COSF(X*EL)))/((A1*A1)+(X*X))
3080         X=A2+A3+A4
3084         W4=((C1*X*SINF(X*EL))+(S1*A1*COSF(X*EL)))/((A1*A1)+(X*X))
3106         VAL=(W1+W2+W3+W4)/(4.)
3115         RETURN
             END
3145         SUBROUTINE SSSS (A1,A2,A3,A4,EL,C1,S1,VAL)
3151         X=A2-A3-A4
3155         W1=((C1*A1*SINF(X*EL))-(S1*X*COSF(X*EL)))/((A1*A1)+(X*X))
3179         X=A2+A3-A4
3183         W2=((C1*A1*SINF(X*EL))-(S1*X*COSF(X*EL)))/((A1*A1)+(X*X))
3207         X=A2-A3+A4
3211         W3=((C1*A1*SINF(X*EL))-(S1*X*COSF(X*EL)))/((A1*A1)+(X*X))
3235         X=A2+A3+A4
3239         W4=((C1*A1*SINF(X*EL))-(S1*X*COSF(X*EL)))/((A1*A1)+(X*X))
3263         VAL=(-W1+W2+W3-W4)/(4.)
3272         RETURN
             END

 CYL SHELL BUC PROB

 GALLERKIN   METHOD
             DIMENSION A(24,24)
3303         K=24
```

```
3306        REWIND 15
3308        READ 450,POI,RAD,E,EL,T,R1,P1,PO,DELP,RO,PR,DPR,PRO
3326    450 FORMAT(7(F10.2,1X))
3328        PI=3.141593
3331        D=(E*(T*T*T))/(12.*(1.-(POI*POI)))
3345    341 R=R1
3347        FK1=10000.0
3349      1 P=P1
3351    151 FK=10.0
3353        DO 4 M=1,K
3357        DO 4 N=1,K
3361        IF(M-N)3,2,3
3365      2 FN=N
3368        A(M,N)= (((EL/2.)*((POI-1.0)/2.)*R*R)-((((FN*PI)/EL)**2)*(EL/2.0))
           1 )/FK
3399        GO TO 4
3400      3 A(M,N)=0.0
3406      4 CONTINUE
3408        WRITE TAPE 15,((A(I,J),I=1,K),J=1,K)
3427        DO 5 M=1,K
3431        DO 5 N=1,K
3435        FN=N
3438        FM=M
3441        X1=((1.+POI)*R*((2.*FN)-1.))/(4.)
3454        X2=(2.*FN)-1.-(2.*FM)
3464        X3=(2.*FN)-1.+(2.*FM)
3472      5 A(M,N )=((X1*(SINF(X2*PI*.5))/X2)-(X1*(SINF(X3*PI*.5))/X3)
           1 )/FK
3499        WRITE TAPE 15,((A(I,J),I=1,K),J=1,K)
3518        DO 6 M=1,K
3522        DO 6 N=1,K
3526        FN=N
3529        FM=M
3532        X1=(1.+POI)*R*FN*.5
3538        X2=(2.*FN)-(2.*FM)+1.0
3548        X3=(2.*FN)+(2.*FM)-1.0
3556      6 A(M ,N)=((X1*SINF(X2*PI*.5)/X2)+(X1*SINF(X3*PI*.5)/X3)      )/FK
3581        WRITE TAPE 15,((A(I,J),I=1,K),J=1,K)
3600        DO 9 M=1,K
3604        DO 9 N=1,K
3608        FN=N
3611        IF (M-N) 18,7,18
3614     18 A(M , N)=0.0
3620        GO TO 9
3621      7 X1=(EL/2.)*R*R
3627        X2=(EL/2.)*(1.-POI)*.5*(PI/(2.*EL))*(PI/(2.*EL))
           1 *(((2.*FN)-1.)**2)
3655      8 A(M , N)=(-X1-X2)     /FK
3664      9 CONTINUE
3666        WRITE TAPE 15,((A(I,J),I=1,K),J=1,K)
3685        Z=((EL*EL*4.)/(RAD*T))*(SQRTF(1.-(POI*POI)))
3702        G1=(.25/EL)*(SQRTF(((4.*SQRTF(3.))*Z)+((P*EL*EL*4.)/D)))
3721        G2=(.25/EL)*(SQRTF(((4.*SQRTF(3.))*Z)-((P*EL*EL*4.)/D)))
3742        Q=((RAD*RAD)/(E*T))*(PR+((POI*P)/RAD))
3757        G22=G2*EL
3760        G33=2.*G22
3763        CALL SINH(G22,0,C16,DUMMY)
```

```
3769       CALL COSH(G22,0,C15,DUMMY)
3775       CALL SINH(G33,0, C11,DUMMY)
3781       Q1=(G1*C11)+(2.*G2*SINF(G1*EL)*COSF(G1*EL))
3796       A11=((-2.)*Q)*((G1*SINF(G1*EL)*C15)-(G2*COSF(G1*EL)*C16))/(Q1)
3821       A22=((-2.)*Q)*((G2*SINF(G1*EL)*C15)+(G1*COSF(G1*EL)*C16))/(Q1)
3844       GA1=(A11*G2)-(A22*G1)
3853       GA2=(A22*G2)+(A11*G1)
3860       GA3=(GA1*G2)-(GA2*G1)
3869       GA4=(GA2*G2)+(GA1*G1)
3876       S1=C16
3878       C1=C15
3880       DO 81 M=1,K
3884       DO 81 N=1,K
3888       FN=N
3891       FM=M
3894       IF(M-N+1) 75,76,75
3898    75 W1=0.0
3900       GO TO 77
3901    76 W1=(.5*(1.-FN)*PI*POI)/RAD
3909    77 IF(M-N)78,79,78
3912    78 W2=0.0
3914       GO TO 80
3915    79 W2=(.5*POI*FN*PI*(-1.))/RAD
3923    80 X1=((FN-1.)*PI)/EL
3929       X2=(FM*PI)/EL
3934       CALL CSCS(G2,G1,X1,X2,EL,C1,S1,X3)
3944       W3=-(((GA1*(FN-1.)*(FN-1.)*PI*PI)/(EL*EL))*X3)-((1.-POI)*
          1 .5*R*R*GA1*X3)
3971       X1=(FN-1.)*PI/EL
3979       X2=FM*PI/EL
3984       CALL SSCC(G2,X2,G1,X1,EL,C1,S1,X3)
3994       X4=GA2*((((FN-1.)*PI)/EL)**2)
4003       X5=(1.-POI)*.5*R*R*GA2
4010       W4=(-1.)*(X4+X5)*X3
4017       X1=FN*PI/EL
4022       X2=FM*PI/EL
4027       CALL CSCS(G2,G1,X1,X2,EL,C1,S1,X3)
4037       X4=GA1*((FN*PI/EL)**2)
4045       X5=(1.-POI)*.5*R*R*GA1
4052       W5=(-X4-X5)*X3
4056       CALL SSCC(G2,X2,G1,X1,EL,C1,S1,X3)
4066       X4=GA2*((FN*PI/EL)**2)
4074       X5=(1.-POI)*.5*R*R*GA2
4081       W6=(-X4-X5)*X3
4085       X1=(FN-1.)*PI/EL
4093       X2=FM*PI/EL
4098       CALL SSSS(G2,G1,X1,X2,EL,C1,S1,X3)
4108       W7=((1.-FN)*PI*GA3/EL)*X3
4118       CALL CSCS(G2,X1,G1,X2,EL,C1,S1,X3)
4128       W8=((1.-FN)*PI*GA4/EL)*X3
4138       X1=FN*PI/EL
4143       CALL SSSS(G2,G1,X1,X2,EL,C1,S1,X3)
4153       W9=((-FN)*PI*GA3/EL)*X3
4162       CALL CSCS(G2,X1,G1,X2,EL,C1,S1,X3)
4172       W10=((-FN)*PI*GA4/EL)*X3
4181    81 A(M,N)=(W1+W2+W3+W4+W5+W6+W7+W8+W9+W10      )/FK
4200       WRITE TAPE 15,((A(I,J),I=1,K),J=1,K)
```

```
4219          DO 85 M=1,K
4223          DO 85 N=1,K
4227          FN=N
4230          FM=M
4233          X1=((2.*FN)-(2.*FM)-(1.))*PI
4246          X2=((2.*FN)+(2.*FM)-(3.))*PI
4259          W1=(R/RAD)*((SINF(X1/2.)/(X1/EL))+(SINF(X2/2.)/(X2/EL)))
4287          X1=(FN-FM+.5)*PI
4292          X2=(FN+FM-.5)*PI
4297          W2=(EL*R/RAD)*((SINF(X1)/(2.*X1))+(SINF(X2)/(2.*X2)))
4320          X1=(FN-1.)*PI/EL
4328          X2=((2.*FM)-1.)*PI/(2.*EL)
4338          CALL SSCC(G2,G1,X1,X2,EL,C1,S1,X3)
4348          W3=(1.-POI)*.5*R*GA3*X3
4355          X1=FN*PI/EL
4360          CALL SSCC(G2,G1,X1,X2,EL,C1,S1,X3)
4370          W4=(1.-POI)*.5*R      *GA3*X3
4377          X1=(FN-1.)*PI/EL
4385          CALL CCCC(G2,G1,X1,X2,EL,C1,S1,X3)
4395          W5=(1.-POI)*.5*R*GA4*X3
4402          X1=FN*PI/EL
4407          CALL CCCC(G2,G1,X1,X2,EL,C1,S1,X3)
4417          W6=(1.-POI)*.5*R*GA4*X3
4424          X1=(FN-1.)*PI/EL
4432          CALL CSCS (G2,G1,X2,X1,EL,C1,S1,X3)
4442          W7=((1.+POI)*.5*R*(1.-FN)*PI*GA1/EL)*X3
4458          CALL SSCC(G2,X1,G1,X2,EL,C1,S1,X3)
4468          W8=((1.+POI)      *.5*R*(1.-FN)*PI*       GA2/EL)*X3
4484          X1=FN*PI/EL
4489          CALL CSCS(G2,G1,X2,X1,EL,C1,S1,X3)
4499          W9=(((-1.)*(1.+POI)*.5*R*FN*PI*GA1)/EL)*X3
4513          CALL SSCC(G2,X1,G1,X2,EL,C1,S1,X3)
4523          W10=(((-1.)*(1.+POI)*.5*R*FN*PI*GA2)/EL)*X3
4537       85 A(M,N)=(W1+W2+W3+W4+W5+W6+W7+W8+W9+W10)/FK
4556          WRITE TAPE 15,((A(I,J),I=1,K),J=1,K)
4575          FK=FK1
4577          DO 90 M=1,K
4581          DO 90 N=1,K
4585          FN=N
4588          FM=M
4591          IF(M-N)87,86,87
4594       87 IF(M-N-1)88,86,88
4599       86 W1=(POI*E*T*FN*PI)/(2.*RAD*(1.-(POI*POI)))
4615          GO TO 89
4616       88 W1=0.0
4618       89 X1=FN*PI/EL
4623          X2=(FM-1.)*PI/EL
4631          CALL SSCC(G2,G1,X1,X2,EL,C1,S1,X3)
4641          X2=FM*PI/EL
4646          CALL SSCC(G2,G1,X1,X2,EL,C1,S1,X4)
4656          W2=((-1.)*(E*T*FN*PI*GA3))/((1.-(POI*POI))*EL)
4674          W2=W2*(X3+X4)
4678          CALL CCCC(G2,G1,X1,X2,EL,C1,S1,X3)
4688          X2=((FM-1.)*PI)/EL
4694          CALL CCCC(G2,G1,X1,X2,EL,C1,S1,X4)
4704          W3=((-1.)*E*T*GA4*FN*PI)/((1.-(POI*POI))*EL)
4720          W3=W3*(X3+X4)
```

```
4724    90 A(M ,N)=(W1+W2+W3)/FK
4736       WRITE TAPE 15,((A(I,J),I=1,K),J=1,K)
4755       DO 91 M=1,K
4759       DO 91 N=1,K
4763       FN=N
4766       FM=M
4769       X1=(2.*FM)-(2.*FN)-1.
4779       W1=(SINF((.5)*PI*X1))/(X1*PI/EL)
4791       X2=(2.*FM)+(2.*FN)-3.
4799       W2=(SINF(PI*.5*X2))/(X2*PI/EL)
4811       X1=FM-FN+.5
4815       W3=(SINF(PI*X1))/(PI*2.*X1/EL)
4829       X1=FM+FN-.5
4833       W4=(SINF(PI*X1))/(PI*2.*X1/EL)
4847       W11=((-1.)*E*T*R)/(RAD*(1.-(POI*POI)))
4861       W1=W11*(W1+W2+W3+W4)
4867       X1=((2.*FN)-1.)*PI/(2.*EL)
4877       X2=(FM-1.)*PI/EL
4885       CALL SSCC(G2,G1,X1,X2,EL,C1,S1,X3)
4895       X2=FM*PI/EL
4900       CALL SSCC(G2,G1,X1,X2,EL,C1,S1,X4)
4910       W2=(E*T*POI*R*GA3*(X3+X4))/(1.-(POI*POI))
4926       CALL CCCC(G2,G1,X1,X2,EL,C1,S1,X3)
4936       X2=(FM-1.)*PI/EL
4944       CALL CCCC(G2,G1,X1,X2,EL,C1,S1,X4)
4954       W3=(E*T*POI*R*GA4*(X3+X4))/(1.-(POI*POI))
4970    91 A(M , N)=(W1+W2+W3)/FK
4982       WRITE TAPE 15,((A(I,J),I=1,K),J=1,K)
5001       G22=2.*G2
5004       G11=2.*G1
5007       GL2=G22*EL
5010       CALL COSH (GL2,0.0,C11,DUMMY)
5016       CALL SINH (GL2,0.0,S11,DUMMY)
5022       C111=C1
5024       S111=S1
5026       DO 131 M=1,K
5030       DO 131 N=1,K
5034       FN=N
5037       FM=M
5040       IF (M-N) 93,92,93
5043    93 IF(M-N+1)94,92,94
5048    92 W1=((((FN-1.)*PI)/EL)**4)*D*EL*.5
5059       GO TO 95
5060    94 W1=0.0
5062    95 IF(M-N)97,96,97
5065    97 IF(M-N-1)98,96,98
5070    96 W2=((FN*PI/EL)**4)*D*EL*.5
5080       GO TO 99
5081    98 W2=0.0
5083    99 IF(M-N)101,100,101
5086   101 IF(M-N+1)102,100,102
5091   100 W3=2.*R*R*D*EL*.5*(((FN-1.)*PI/EL)**2)
5107       GO TO 103
5108   102 W3=0.0
5110   103 IF(M-N)105,104,105
5113   105 IF(M-N-1)106,104,106
5118   104 W4=2.*R*R*D*EL*.5*FN*FN*PI*PI/(EL*EL)
```

```
5132          GO TO 107
5133      106 W4=0.0
5135      107 X1=(E*T)/((1.-(POI-POI))*RAD*RAD)
5148          X2=D*(R**4)
5153          X1=X1+X2
5156          CALL SSCC(G22,X1,0.0,X2,EL,C1,S1,X3)
5166      108 IF(M-N)110,109,110
5170      109 W5=X1*EL
5173          GO TO 111
5174      110 W5=0.0
5176      111 IF(M-N+1)113,112,113
5180      113 IF(M-N-1)114,112,114
5185      112 W5A=X1*EL*.5
5189          GO TO 115
5190      114 W5A=0.0
5192      115 Y1=(        POI*E*T*GA1*PI)/(RAD*(1.-(POI*POI)))
5207          X1=(FN-1.)*PI/EL
5215          X2=(FM-1.)*PI/EL
5223          CALL CSCS(G2,G1,X2,X1,EL,C1,S1,X3)
5233          X2=FM*PI/EL
5238          CALL CSCS(G2,G1,X2,X1,EL,C1,S1,X4)
5248          X1=FN*PI/EL
5253          X2=(FM-1.)*PI/EL
5261          CALL CSCS(G2,G1,X2,X1,EL,C1,S1,X5)
5271          X2=FM*PI/EL
5276          CALL CSCS(G2,G1,X2,X1,EL,C1,S1,X6)
5286          W6=(((1.-FN)/EL)*Y1*(X3+X4))-(((FN    /EL)*Y1)*(X5+X6))
5308          Y=E*(-1.)*POI*T*GA2*PI/(RAD*(1.-(POI*POI))*EL)
5327          X1=(FN-1.)*PI/EL
5335          X2=(FM-1.)*PI/EL
5343          CALL SSCC(G2,X1,G1,X2,EL,C1,S1,X3)
5353          X2=FM*PI/EL
5358          CALL SSCC(G2,X1,G1,X2,EL,C1,S1,X4)
5368          X1=FN*PI/EL
5373          X2=(FM-1.)*PI/EL
5381          CALL SSCC(G2,X1,G1,X2,EL,C1,S1,X5)
5391          X2=FM*PI/EL
5396          CALL SSCC(G2,X1,G1,X2,EL,C1,S1,X6)
5406          W7=((FN-1.)*Y*(X3+X4))+(FN*Y*(X5+X6))
5420          IF(M-N)117,116,117
5423      117 IF(M-N+1)118,116,118
5428      116 W8=(-P)*((((FN-1.)*PI)/EL)**2)*EL*.5
5441          GO TO 119
5442      118 W8=0.0
5444      119 IF(M-N)121,120,121
5447      121 IF(M-N-1)122,120,122
5452      120 W9=(-P)*((FN*PI/EL)**2)*EL*.5
5464          GO TO 123
5465      122 W9=0.0
5467      123 IF(M-N)125,124,125
5471      124 W10=(E*T*R*R*Q*EL/RAD)-(POI*P*R*R*EL)
5491          GO TO 126
5492      125 W10=0.0
5494      126 IF(M-1-N)128,127,128
5498      128 IF(M+1-N)129,127,129
5503      127 W10A=((E*T*R*R*Q/RAD)-(POI*P*R*R)).*EL*.5
5523          GO TO 130
```

```
  129 W10A=0.0
  130 C1=C11
      S1=S11
      X1=(FN-1.)*PI/EL
      X2=(FM-1.)*PI/EL
      X2=FM*PI/EL
      CALL SSCC(G22,X1,0.0,X2,EL,C1,S1,X4)
      CALL SSCC(G22,X1,G11,X2,EL,C1,S1,X6)
      X2=(FM-1.)*PI/EL
      CALL SSCC(G22,X1,G11,X2,EL,C1,S1,X5)
      X10=(E*T*GA1*GA3*PI)/(4.*EL*(1.-(POI*POI)))
      W15A=(FN-1.)*X10*(X3+X4-X5-X6)
      X1=FN*PI/EL
      CALL SSCC(G22,X1,G11,X2,EL,C1,S1,X3)
      CALL SSCC(G22,X1,0.0,X2,EL,C1,S1,X5)
      X2=FM*PI/EL
      CALL SSCC(G22,X1,G11,X2,EL,C1,S1,X4)
      CALL SSCC(G22,X1,0.0,X2,EL,C1,S1,X6)
      W15B=FN*X10*(X3+X4-X5-X6)     *(-1.)
      W15=W15A+W15B
      X10=E*T*GA2*GA3*PI/(4.*EL*(1.-(POI*POI)))
      X1=(FN-1.)*PI/EL
      X2=(FM-1.)*PI/EL
      CALL CSCS(G22,G11,X2,X1,EL,C1,S1,X3)
      CALL CSCS(0.0,G11,X2,X1,EL,1.0,0.0,X5)
      X2=(PI/EL)*FM
      CALL CSCS(G22,G11,X2,X1,EL,C1,S1,X4)
      CALL CSCS(0.0,G11,X2,X1,EL,1.0,0.0,X6)
      W16A=(FN-1.)*X10*(X3+X4-X5-X6)
      X1=FN*PI/EL
      CALL CSCS(G22,G11,X2,X1,EL,C1,S1,X4)
      CALL CSCS(0.0,G11,X2,X1,EL,1.0,0.0,X6)
      X2=(FM-1.)*PI/EL
      CALL CSCS(G22,G11,X2,X1,EL,C1,S1,X3)
      CALL CSCS( 0.0,G11,X2,X1,EL,1.0,0.0,X5)
      W16B=FN*X10*(X3+X4-X5-X6)
      W16=W16A+W16B
      X10=E*T*GA1*GA4*PI/(4.*EL*(1.-(POI*POI)))
      X1=(FN-1.)*PI/EL
      CALL CSCS(G22,G11,X2,X1,EL,C1,S1,X3)
      CALL CSCS(0.0,G11,X2,X1,EL,1.0,0.0,X5)
      X2=FM*PI/EL
      CALL CSCS(G22,G11,X2,X1,EL,C1,S1,X4)
      CALL CSCS(0.0,G11,X2,X1,EL,1.0,0.0,X6)
      W17A=X10*(FN-1.)*(X3+X4+X5+X6)
      X1=FN*PI/EL
      CALL CSCS(G22,G11,X2,X1,EL,C1,S1,X4)
      CALL CSCS(0.0,G11,X2,X1,EL,1.0,0.0,X6)
      X2=(FM-1.)*PI/EL
      CALL CSCS(G22,G11,X2,X1,EL,C1,S1,X3)
      CALL CSCS(0.0,G11,X2,X1,EL,1.0,0.0,X5)
      W17B=FN*X10*(X3+X4+X5+X6)
      W17=W17A+W17B
      X10=E*T*GA2*GA4*PI/(4.*(1.-(POI*POI)))
      X1=(FN-1.)*PI/EL
      X2=(FM-1.)*PI/EL
      CALL SSCC(G22,X1,0.0,X2,EL,C1,S1,X3)
```

```
      CALL SSCC(G22,X1,G11,X2,EL,C1,S1,X5)
      X2=FM*PI/EL
      CALL SSCC(G22,X1,0.0,X2,EL,C1,S1, X4)
      CALL SSCC(G22,X1,G11,X2,EL,C1,S1,X6)
      W18A=(FN-1.)*X10*(X3+X4+X5+X6)    /EL
      X1=FN*PI/EL
      X2=(FM-1.)*PI/EL
      CALL SSCC(G22,X1,0.0,X2,EL,C1,S1,X3)
      CALL SSCC(G22,X1,G11,X2,EL,C1,S1,X5)
      X2=FM*PI/EL
      CALL SSCC(G22,X1,0.0,X2,EL,C1,S1,X4)
      CALL SSCC(G22,X1,G11,X2,EL,C1,S1,X6)
      W18B=FN*X10*(X3+X4+X5+X6)     /EL
      W18=W18A+W18B
      C1=C111
      S1=S111
      X10=E*T*R*R*A11/RAD
      X1=(FN-1.)*PI/EL
      X2=(FM-1.)*PI/EL
      CALL SSCC(G2,G1,X1,X2,EL,C1,S1,X3)
      X2=FM*PI/EL
      CALL SSCC(G2,G1,X1,X2,EL,C1,S1,X4)
      X1=FN*PI/EL
      CALL SSCC(G2,G1,X1,X2,EL,C1,S1,X6)
      X2=(FM-1.)*PI/EL
      CALL SSCC(G2,G1,X1,X2,EL,C1,S1,X5)
      W11=X10*(X3+X4+X5+X6)
      X10=E*T*R*R*A22/RAD
      CALL CCCC(G2,G1,X1,X2,EL,C1,S1,X5)
      X2=FM*PI/EL
      CALL CCCC(G2,G1,X1,X2,EL,C1,S1,X6)
      X1=(FN-1.)*PI/EL
      CALL CCCC(G2,G1,X1,X2,EL,C1,S1,X4)
      X2=(FM-1.)*PI/EL
      CALL CCCC(G2,G1,X1,X2,EL,C1,S1,X3)
      W12=X10*(X3+X4+X5+X6)
      X10=((-1.)*E*T*GA3)/(RAD*(1.-(POI*POI)))
      CALL SSCC(G2,G1,X1,X2,EL,C1,S1,X3)
      X2=FM*PI/EL
      CALL SSCC(G2,G1,X1,X2,EL,C1,S1,X4)
      X1=FN*PI/EL
      X2=(FM-1.)*PI/EL
      CALL SSCC(G2,G1,X1,X2,EL,C1,S1,X6)
      CALL SSCC(G2,G1,X1,X2,EL,C1,S1,X5)
      W13=X10*(X3+X4+X5+X6)*POI
      X10=((-1.)*E*T*GA4)/(RAD*(1.-(POI*POI)))
      CALL CCCC(G2,G1,X1,X2,EL,C1,S1,X5)
      X2=FM*PI/EL
      CALL CCCC(G2,G1,X1,X2,EL,C1,S1,X6)
      X1=(FN-1.)*PI/EL
      CALL CCCC(G2,G1,X1,X2,EL,C1,S1,X4)
      X2=(FM-1.)*PI/EL
      CALL CCCC(G2,G1,X1,X2,EL,C1,S1,X3)
      W14=X10*(X3+X4+X5+X6)*POI
  131 A(M , N)=         (W1+W2+W3+W4+W5+W5A+W6+W7+W8+W9+W10+W10A+
     1 W11+W12+W13+W14+W15+W16+W17+W18)/FK
      WRITE TAPE 15,((A(I,J),I=1,K),J=1,K)
```

```
6502          P=P+DELP
6505          IF (P-PO) 151,337,151
6509      337 IF (R-RO) 338,339,338
6512      338 R=R+2.0
6515          GO TO 1
6516      339 IF (PR-PRO) 340,336,340
6519      340 PR=PR+DPR
6522          GO TO 341
6523      336 PRINT 470,POI,RAD,E,EL,T,R,PR
6534          END FILE 15
6536          REWIND 15
6539      470 FORMAT (10(F10.2,1X))
6541          STOP
              END

SUBROUTINE     CADD

VARIABLES
 NAME LOC.
AI     0000      AR     0000      BI     0000      BR     0000      CI     0000      CR

STATEMENT NUMBERS
STMNT LOC.

...   NONE   ...

SUBROUTINE     CSUBT

VARIABLES
 NAME LOC.
AI     0000      AR     0000      BI     0000      BR     0000      CI     0000      CR

STATEMENT NUMBERS
STMNT LOC.

...   NONE   ...

SUBROUTINE     CMULT

VARIABLES
 NAME LOC.
AI     0000      A1     2115      BI     0000      B1     2117      CI     0000
AR     0000      A2     2116      BR     0000      B2     2118      CR     0000

STATEMENT NUMBERS
STMNT LOC.

...   NONE   ...

SUBROUTINE     CDIV

VARIABLES
 NAME LOC.
AI     0000      A1     2192      BI     0000      B1     2194      CI     0000      D
AR     0000      A2     2193      BR     0000      B2     2195      CR     0000

STATEMENT NUMBERS
```

```
** T THIS PROG,M READS SCRATCH TAPE ON DR 24 LOADED BY PROG,M 1
*    COMPILE FORTRAN,EXECUTE FORTRAN, DUMP IF ERROR                        77
SUBROUTINEDET(A,N,JX,ANS)
   LC DEFINED BUT NOT USED IN AN ARITH STMNT.
   I1 DEFINED BUT NOT USED IN AN ARITH STMNT.
   I2 DEFINED BUT NOT USED IN AN ARITH STMNT.
   MO DEFINED BUT NOT USED IN AN ARITH STMNT.
*** MAIN PROGRAM ***
   KK DEFINED BUT NOT USED IN AN ARITH STMNT.
  JJJ DEFINED BUT NOT USED IN AN ARITH STMNT.
2000          SUBROUTINE DET(A,N,JX,ANS)
              DIMENSION A(1300)
2006          LC=N
2008          LR=N
2010       23 DO 31 L=1,LR
2014          NO=L+JX*(L-1)
2021        3 IF(L-LR)2,4,4

 TEST FOR POSSIBLE ROW INTERCHANGE
2026        2 BIGA=A(NO)
2030          NPN=0
2032          I1=L+1
2035          DO 25 JO=I1,LR
2040          NP=JO+JX*(L-1)
2047          IF(ABSF(BIGA)-ABSF(A(NP)))24,25,25
2056       24 BIGA=A(NP)
2058          NPN=NP
2060       25 CONTINUE

 TEST FOR POSSIBLE COLUMN INTERCHANGE
2061          NPM=0
2063          I2=L+1
2066          DO 52 M=I2,LC
2071          NZ = L+JX*(M-1)
2078          IF(ABSF(BIGA)-ABSF(A(NZ))) 51,52,52
2087       51 NPM=NZ
2089          BIGA=A(NZ)
2091       52 CONTINUE
2092          IF(NPM) 55,54,55
2095       54 IF(NPN) 27,4,27

 INTERCHANGE COLUMNS
2098       55 DO 56 K=L,LC
2103          NQ = K+(L-1)*JX
2109          NU = NPM+(K-L)
2115          C = -A(NQ)
2119          A(NQ) = A(NU)
2123       56 A(NU) = C
2126          GO TO 4

 INTERCHANGE ROWS
2127       27 DO 26 K=L,LC
2132          NQ = L+JX*(K-1)
2139          C=-A(NQ)
2143          NU = NPN-(L-1)*JX+JX*(K-1)
2157          A(NQ)=A(NU)
2161       26 A(NU)=C
2164        4 DIVA=1.0/A(NO)
```

```
'TEST FOR COMPUTATIONAL SINGULARITY
2170          IF DIVIDE CHECK 6,11
2172        6 SENSE LIGHT 4
2173          PRINT 16,L,A(NO)
2181       16 FORMAT(12HERROR IN ROWI3,21H OF SIMEQ-DIVIDING BY E16.8)
2191          ANS=.99999999E49
2193          RETURN
2194       11 IF(L-LR)12,42,42

 MATRIX TRANSFORMATION
2199       12 MO=L+1
2202          DO 28 J=MO,LC
2207          NR=L+JX*(J-1)
2214       28 A(NR)=A(NR)*DIVA
2220       29 I1=L+1
2223          DO 31 I=I1,LR
2228          NS=I+JX*(L-1)
2235          FMLTA=A(NS)
2239          DO 31 J=L,LC
2244          NT=I+JX*(J-1)
2251          NY=L+JX*(J-1)
2258       31 A(NT)=A(NT)-A(NY)*FMLTA

 COMPUTE THE DETERMINATE = PI OF A(I,I)
2269       42 ANS=1.0
2271          DO 44 I=1,N
2275          NV=I+JX*(I-1)
2282       44 ANS=ANS*A(NV)
2288          RETURN
              END

 CYL SHELL PROB

GALERKIN METHOD
              DIMENSION A(72,72)
2340          K=24
2343          KK=2*K
2346          KKK=3*K
2349          X=0.0
2351          Y=4.0
2353        9 READ TAPE 15 ,((A(I,J),I=1,K),J=1,K)
2372          JJ=K+1
2375        1 READ TAPE 15, ((A(I,J),I=1,K),J=JJ,KK)
2395        2 READ TAPE 15, ((A(I,J),I=JJ,KK),J=1,K)
2415        3 READ TAPE 15, ((A(I,J),I=JJ,KK),J=JJ,KK)
2436          JJJ=JJ+K
2439        4 READ TAPE 15, ((A(I,J),I=1,K),J=JJJ,KKK)
2459        5 READ TAPE 15, ((A(I,J),I=JJ,KK),J=JJJ,KKK)
2480        6 READ TAPE 15, ((A(I,J),I=JJJ,KKK),J=1,K)
2500        7 READ TAPE 15, ((A(I,J),I=JJJ,KKK),J=JJ,KK)
2521        8 READ TAPE 15, ((A(I,J),I=JJJ,KKK),J=JJJ,KKK)
2542          CALL DET (A,KKK,KKK,ANS)
2548          PRINT 333, ANS
2554      333 FORMAT (2E20.8)
2555          X=X+1.
2559          IF (X-Y) 9,10,9
```

```
2563     10 REWIND 15
2565        STOP
            END
```

SUBROUTINE DET

VARIABLES

NAME	LOC.									
A	0000	DIVA	2327	I2	2320	K	2323	M	2321	NP
ANS	0000	FMLTA	2333	J	2329	L	2312	MO	2328	NPM
BIGA	2314	I	2331	JO	2317	LC	2310	N	0000	NPN
C	2326	I1	2316	JX	0000	LR	2311	NO	2313	NQ

STATEMENT NUMBERS

STMNT	LOC.									
2	2026	6	2172	16	2181	25	2060	28	2214	4:
3	2021	11	2194	23	2010	26	2161	29	2220	4
4	2164	12	2199	24	2056	27	2127	31	2258	5

MAIN PROGRAM

VARIABLES

NAME	LOC.									
A	2568	I	7758	JJ	7759	K	7752	KKK	7754	Y
ANS	7761	J	7757	JJJ	7760	KK	7753	X	7755	

STATEMENT NUMBERS

STMNT	LOC.									
1	2375	3	2415	5	2459	7	2500	9	2353	33:
2	2395	4	2439	6	2480	8	2521	10	2563	

HIGHEST ADDRESS ASSIGNED 7772

BIBLIOGRAPHY

1. Timoshenko, S. and Gere, J., "Theory of Elastic Stability," McGraw Hill Book Co., 2nd ed., pp. 462-466.

2. Donnell, L. H., "A New Theory for the Buckling of Thin Cylinders under Axial Compression and Bending," ASME Transactions, vol. 56, pp. 795-806.

3. Lundquist, E., "Strength Tests of Thin-Walled Duralumin Cylinders in Compression," NACA Rep. 473, 1933.

4. Donnell, L. H. and Wan, C. C., "Effect of Imperfections on Buckling of Thin Cylinders and Columns under Axial Compression," J. Applied Mechanics, vol. 17, No. 1, p. 73, 1950.

5. Flügge, W., "Die Stabilitaet der Kreiszylinderschale," Ing. Arch. vol. 3, pp. 463, 1932.

6. Von Kármán, T. and Tsien, H. S., "The Buckling of Thin Cylindrical Shells under Axial Compression," J. Aeronaut. Sci., vol. 8, No. 8, pp. 302-313.

7. Yoshimura, Y., "On the Mechanism of Buckling of a Circular Cylindrical Shell under Axial Compression," NACA TM 1390, 1955.

8. Thielemann, W., "On the Postbuckling Behavior of Thin Cylindrical Shells," NASA, TND-1510, 1962.

9. Uemura, M., "Postbuckling Behavior of a Circular Cylindrical Shell that Buckles Locally under Axial Compression," Department of Aeronautics and Astronautics, Stanford University, S.U.D.A.E.R. No. 56, 1963.

10. Evan-Iwanowski, R. M., Loo, T. C. and Tierney, D. H., "Local Buckling of Shells," Proceedings. 8th Midwestern Mechanics Conference April 3-4, 1963, Case Institute of Technology, Cleveland, Ohio. Developments in Mechanics, vol. 2. pp. 221-251, 1963.

11. Tennyson, R., "A Note on the Classical Buckling Load of Circular Cylindrical Shells under Axial Compression," AIAA Journal 1, pp. 475-476, (1963).

12. Leonard, R.,"Comments on, "A Note on the Classical Buckling Load of Circular Cylindrical Shells under Axial Compression,""AIAA Journal 1, pp. 2194-2195, (1963).

13. Föppl, L., "A Chsensymmetrisches Ausknicken Zylindrischer Schalen," S. B. Bayr. Akad. Wiss. 1926, pp. 27-40.

14. Flügge, W., "Stresses in Shells," Springer-Verlag, Berlin.

15. Stein, M., "The Influence of Prebuckling Deformations and Stresses on the Buckling of Perfect Cylinders," NASA TR R-190, Feb. 1964.

16, Fischer, G., "Uber den Einfluss der gelenkigen Lagerung aur die Stabilitat Dunnwandiger Kreiszylinderschalen unter Axiallast und innendruck," Zeitschr Flugwiss. 11, (1963), 111-119.

17. Koiter, W. T., "The Effect of Axisymmetric Imperfections on the Buckling of Cylindrical Shells under Axial Compression," Lockheed Missiles and Space Co., 1963.

18. Hoff, N., "Buckling of Thin Shells," Department of Aeronautical Engineering, Stanford University, S.U.D.A.E.R. No. 114.

19. Nachbar, W. and Hoff, N., "On Edge Buckling of Axially-Compressed, Circular Cylindrical Shells," Department of Aeronautical Engineering, Stanford University, S.U.D.A.E.R. No. 115.

20. Donnell, L. H., "Stability of Thin-Walled Tubes under Torsion," NACA Report No. 479, 1933.

21. Ohira, H., "Local Buckling Theory of Axially Compressed Cylinders," Proceedings of Eleventh Japan National Congress for Applied Mechanics, 1961.

22. Hoff, N. and Redfield, L., "Buckling of Axially Compressed Circular Cylindrical Shells at Stresses Smaller than the Classical Critical Value," Department of Aeronautical Engineering, Stanford University, S.U.D.A.E.R, No. 191.

23. Almroth, B. O., "Influence of Edge Conditions on the Stability of Axially Compressed Cylindrical Shells," NASA C.R.-161, Feb. 1965.

24. Sobel, L. H., "Effects of Boundary Conditions on the Stability of Cylinders Subject to Lateral and Axial Pressures," Lockheed Missiles and Space Co., Sept. 1963.